Helmholtz Zentrum Berlin

SoNS 2014

Neutron imaging II

Nikolay Kardjilov

Neutron imaging

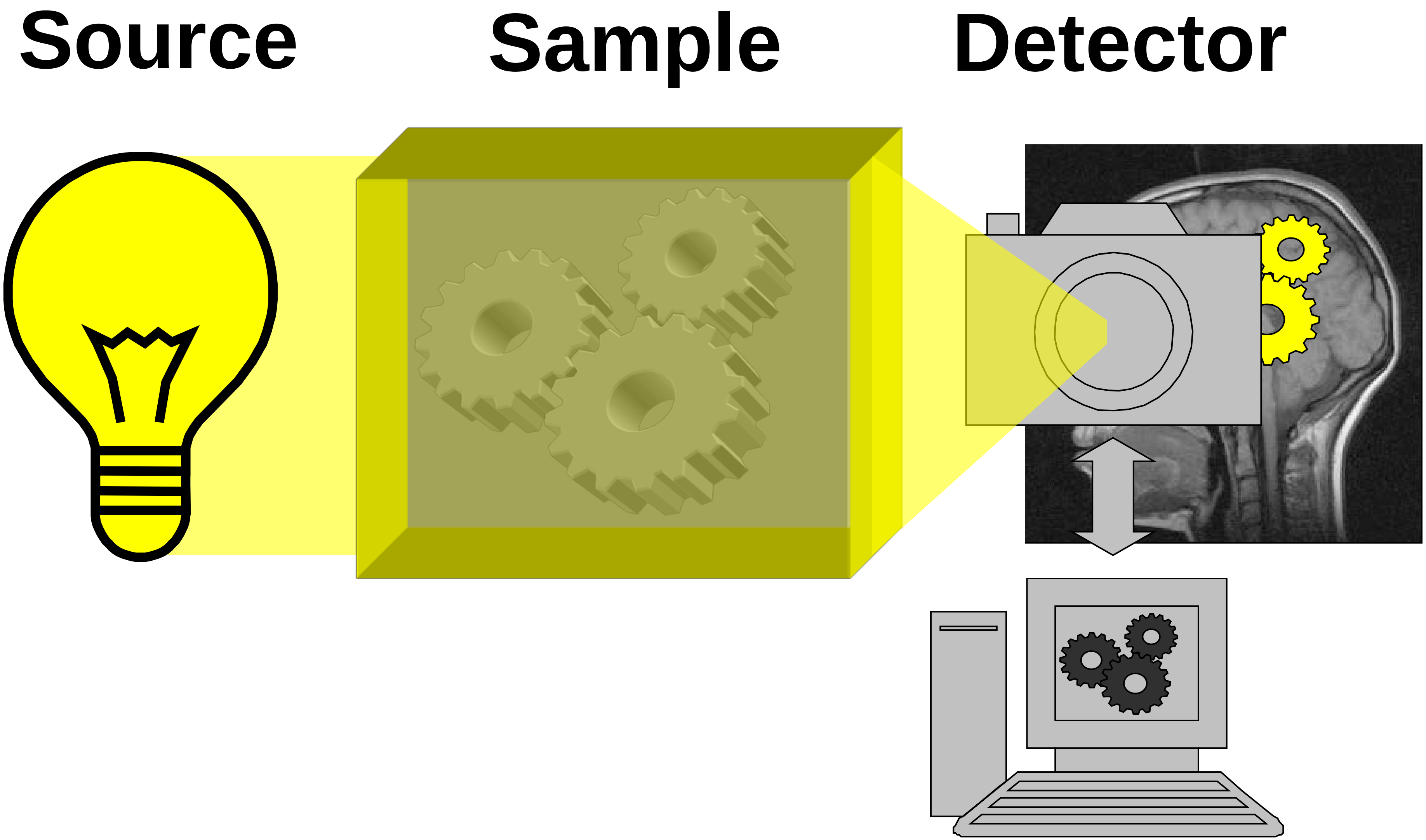

Contrast

Resolution

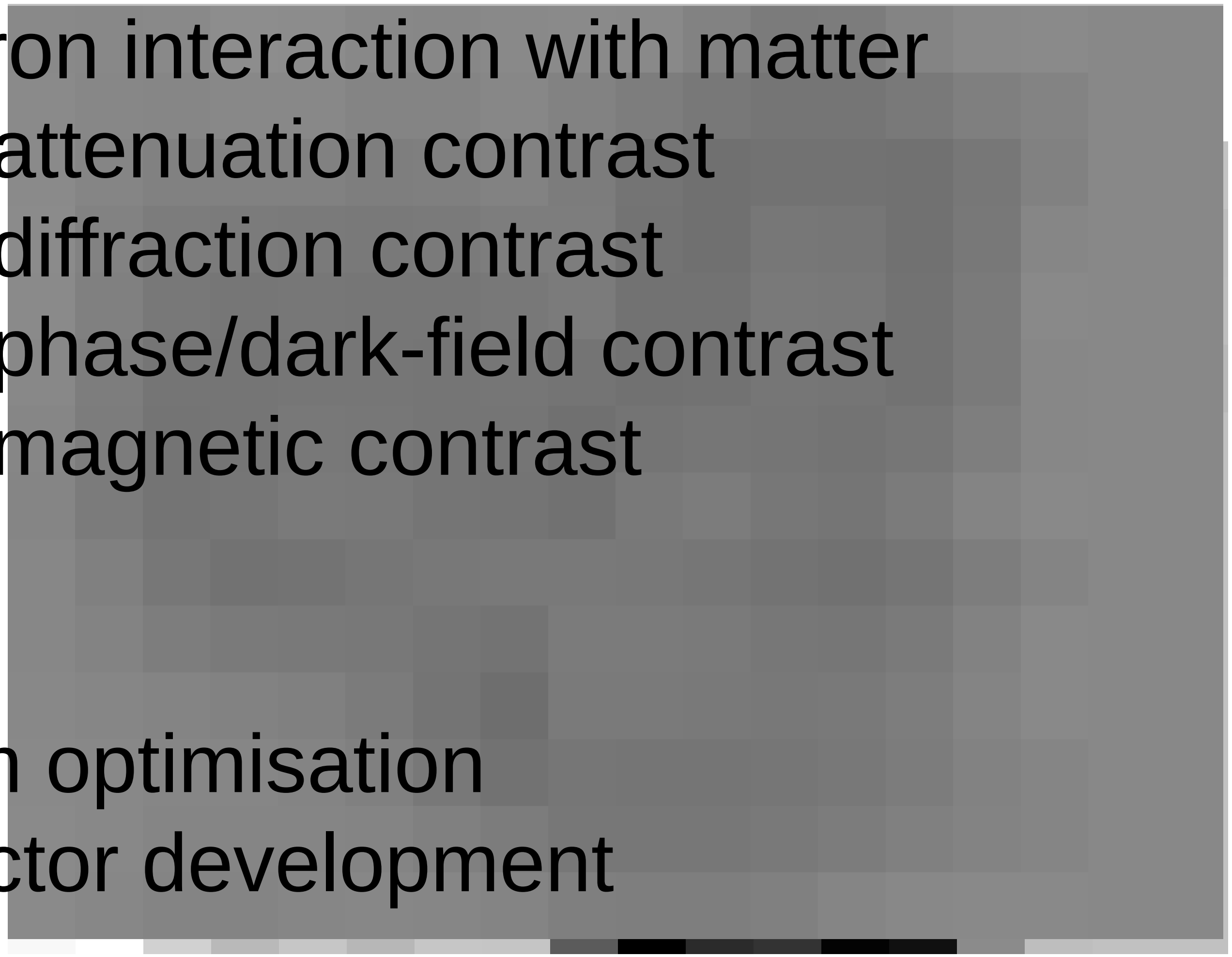

- Neutron interaction with matter
  - attenuation contrast
  - diffraction contrast
  - phase/dark-field contrast
  - magnetic contrast

- Beam optimisation
- Detector development

Attenuation Contrast

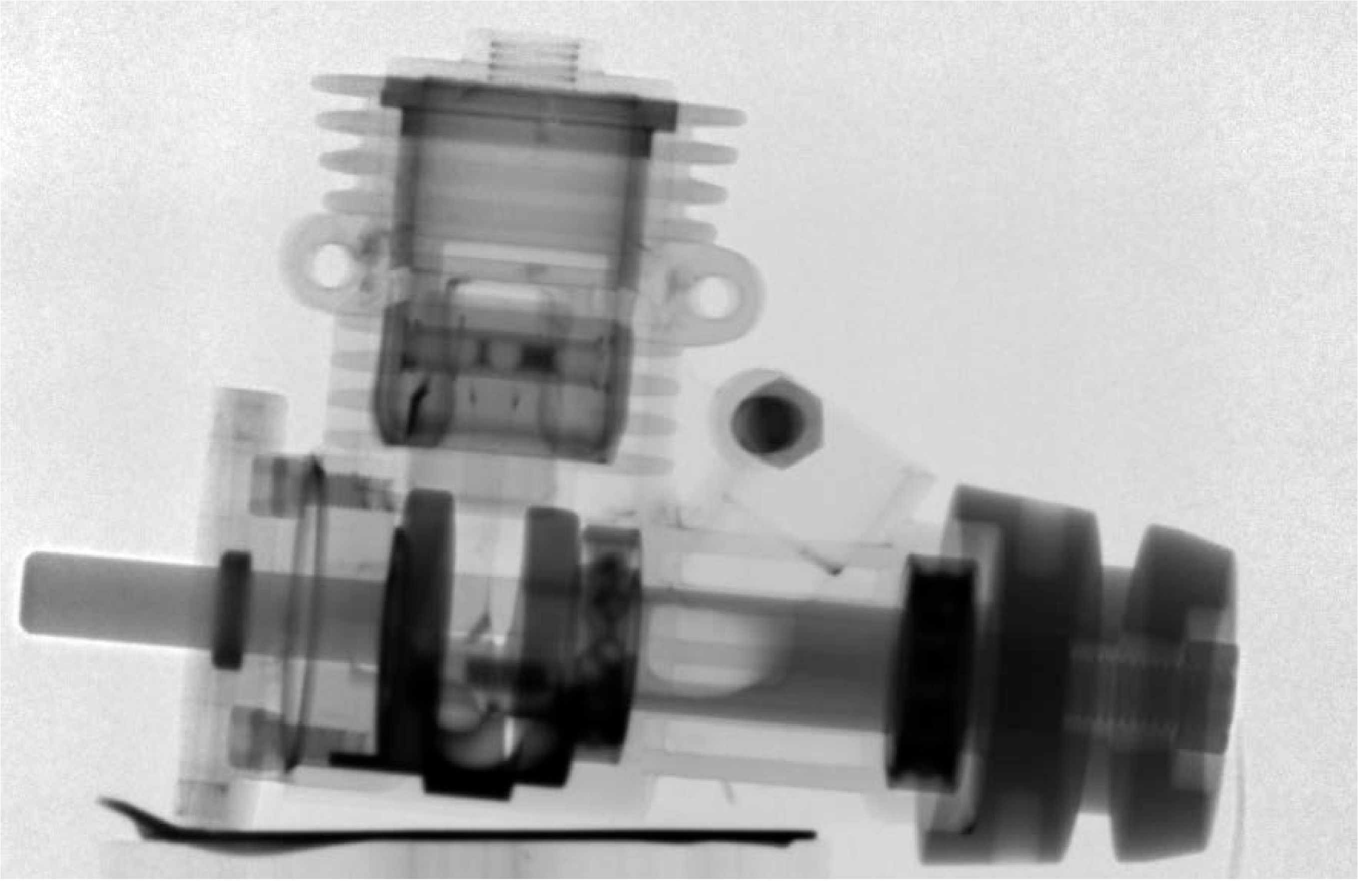

1 cm

Diffraction Contrast

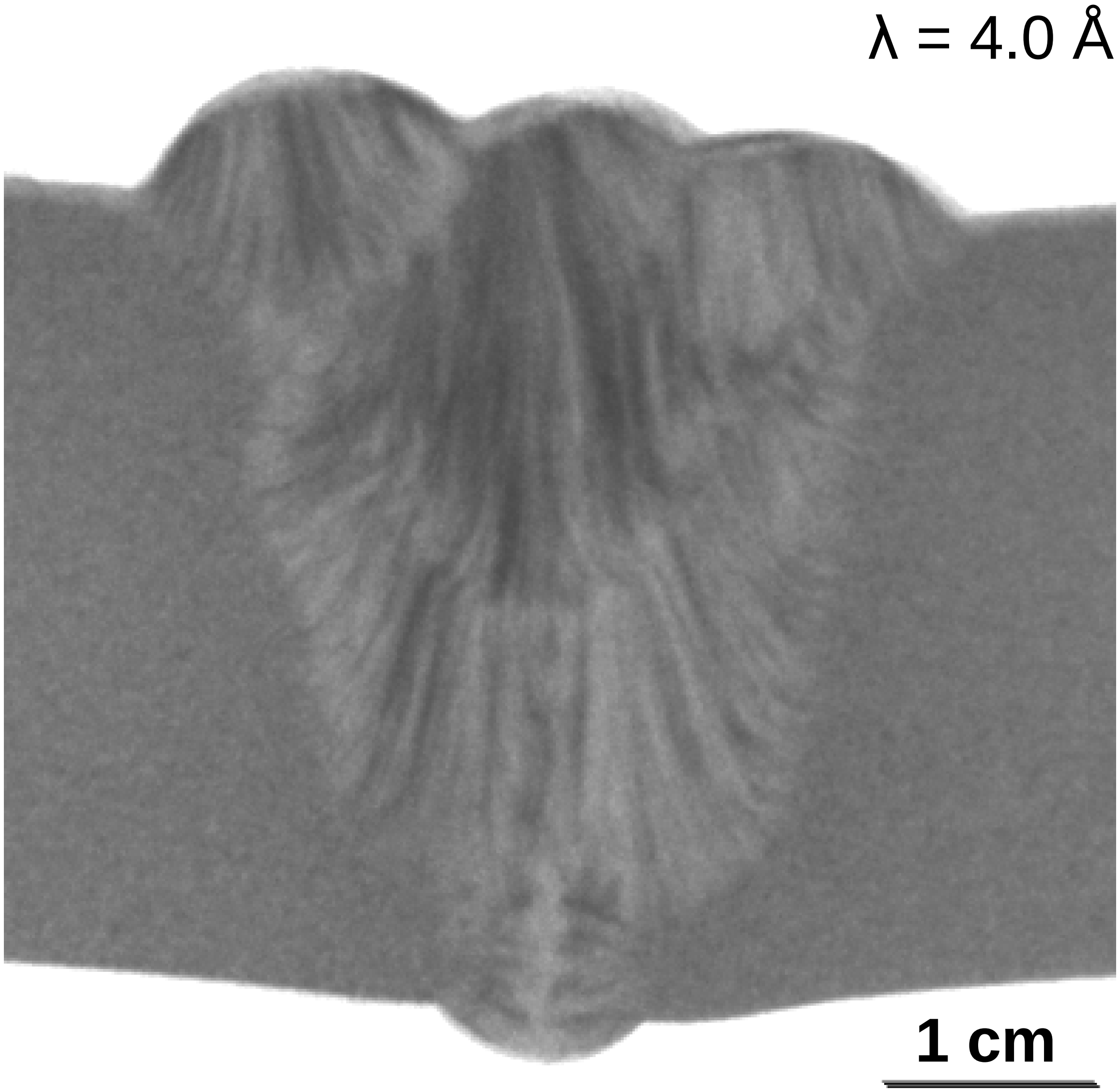

Neutron imaging

Beam monochromatisation

Double crystal monochromator: PCG crystals (mosaicity of 0.8°)

Range: 2.0 – 6.5 Å

Resolution ($\Delta\lambda/\lambda$): ~ 3%

Neutron flux: ~ 4×10^5 n/cm^{2}s (at λ=3.0 Å)

Beam size: 5 x 20 cm^2

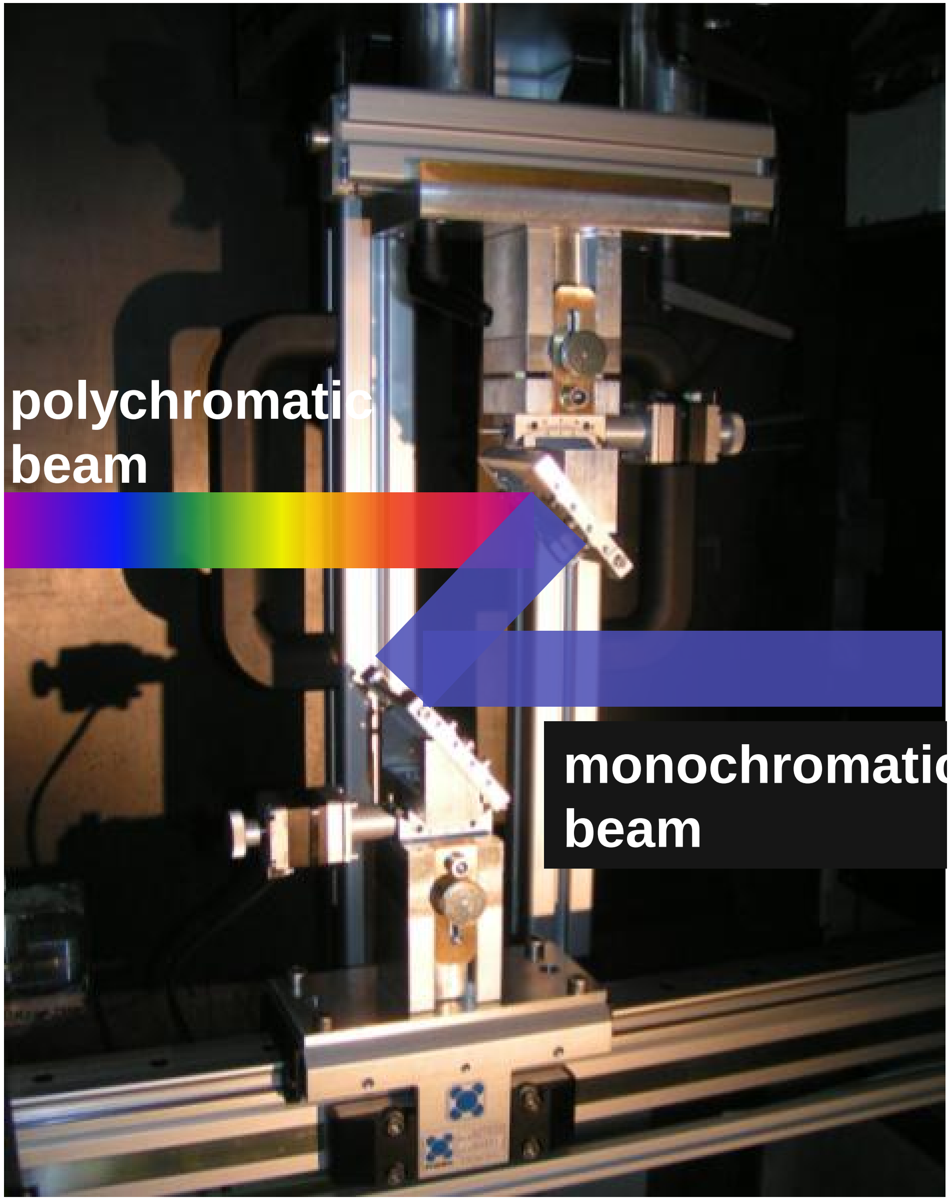

Kardjilov, Nikolay, et al. "New trends in neutron imaging." *Nuclear Instruments and Methods in Physics Research Section A: Accelerators, Spectrometers, Detectors and Associated Equipment* 605.1 (2009): 13-15.

Diffraction Contrast

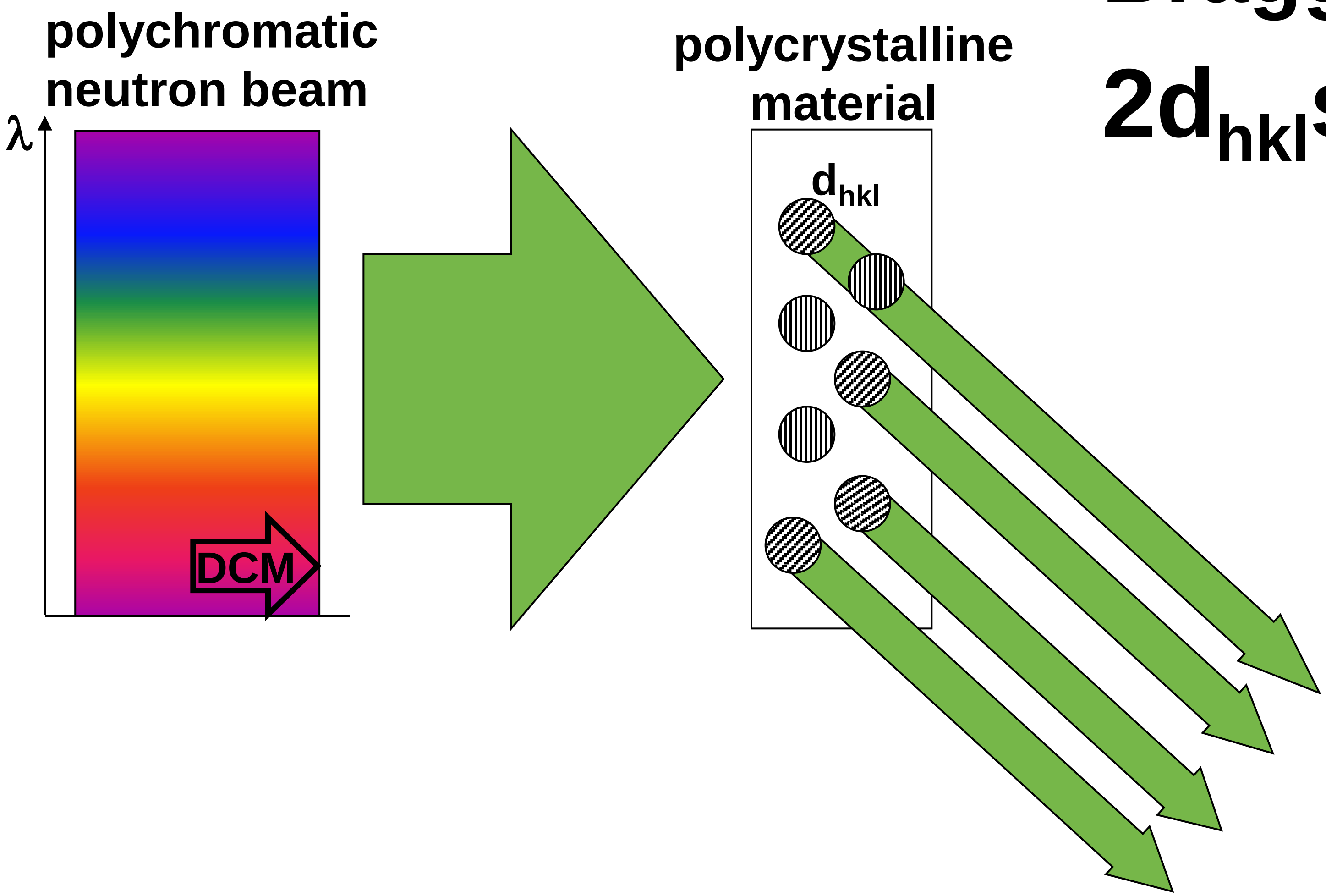

Bragg's law

$$2d_{hkl}\sin\theta=\lambda$$

Diffraction Contrast

polychromatic neutron beam

polycrystalline material

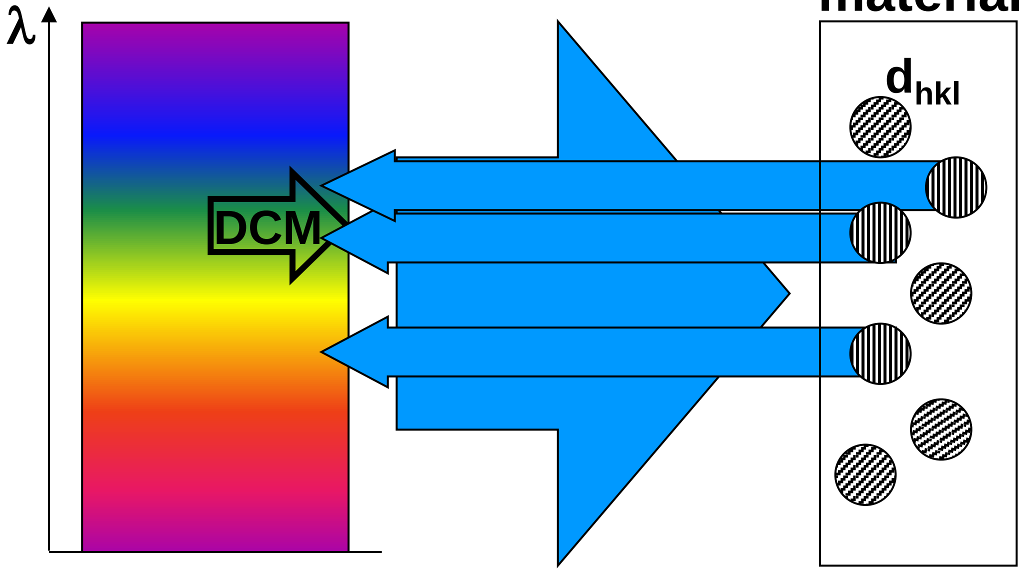

Bragg's law

$$2d_{hkl}\sin 90° = \lambda$$

Cross-sections of iron per ator

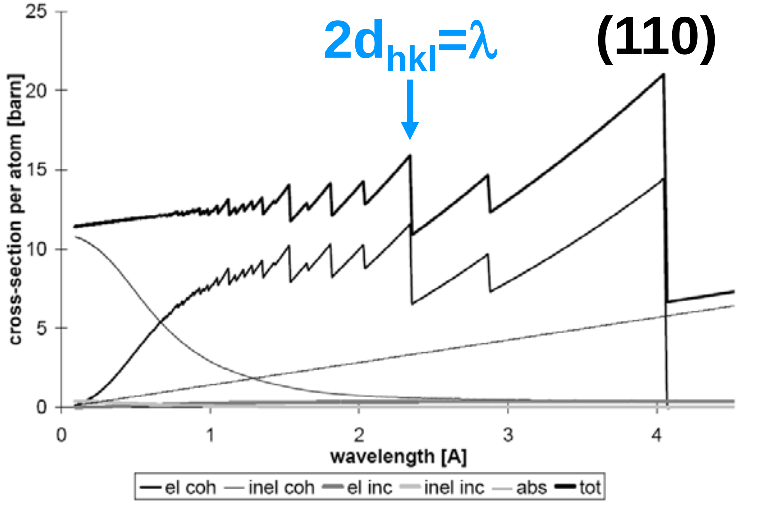

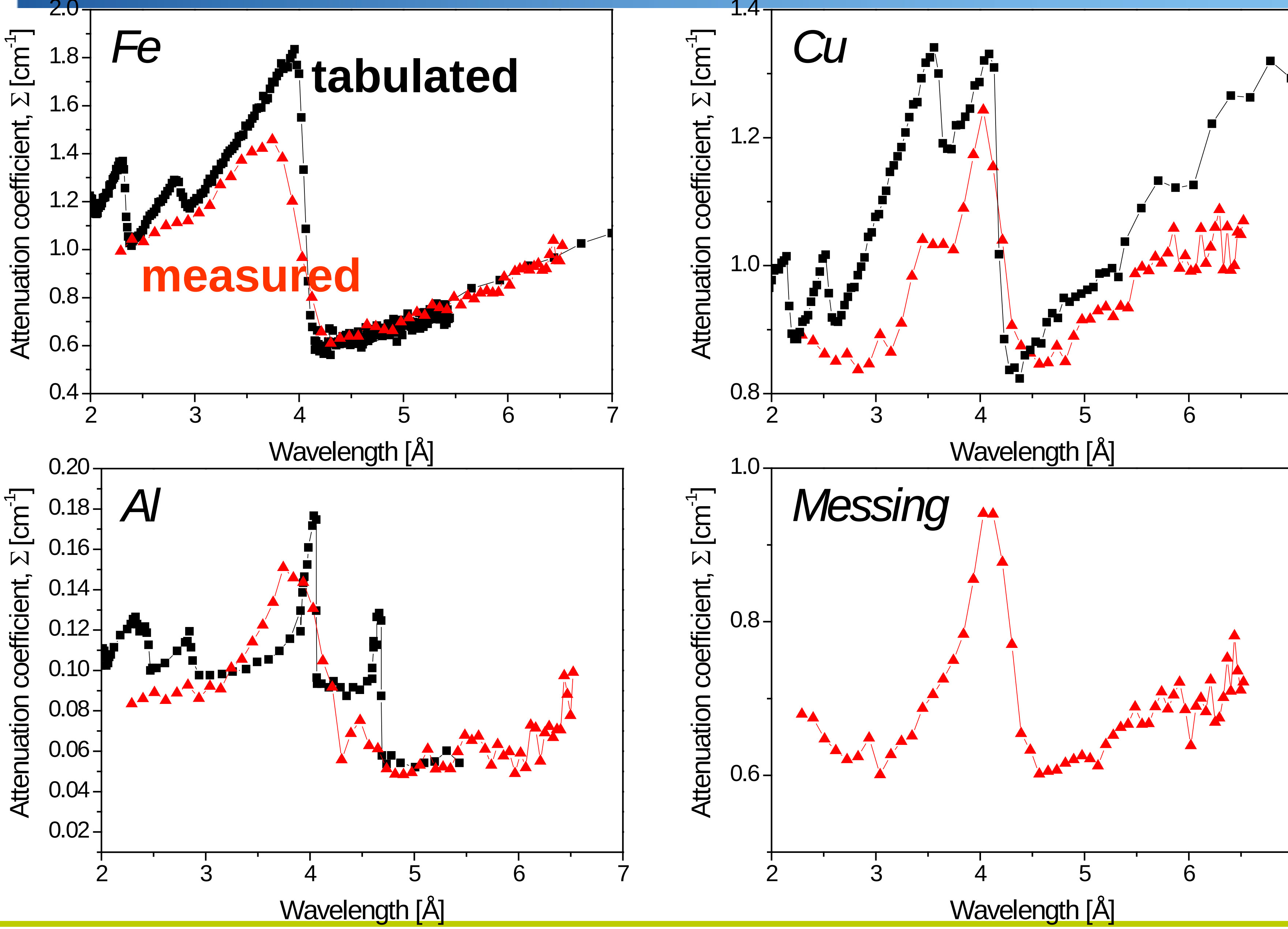
Fe
tabulated
measured
Cu
Al
Messing
Attenuation coefficient, Σ [cm-1]
Wavelength [Å]

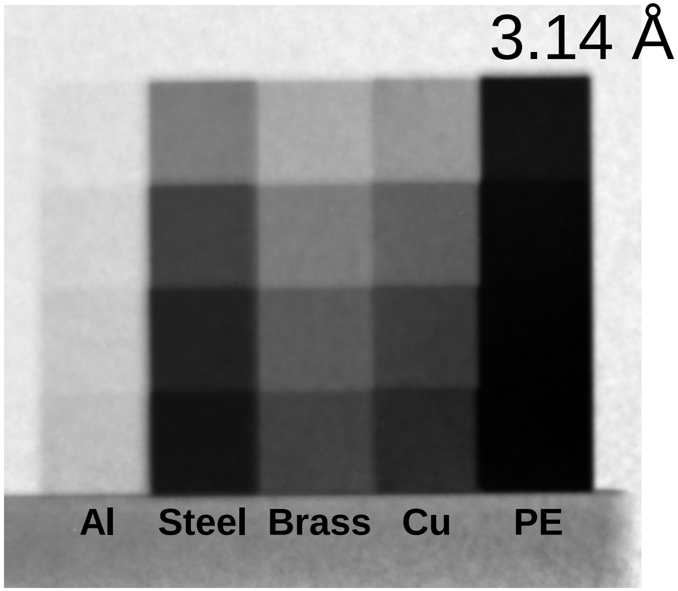
3.14 Å
Al Steel Brass Cu PE

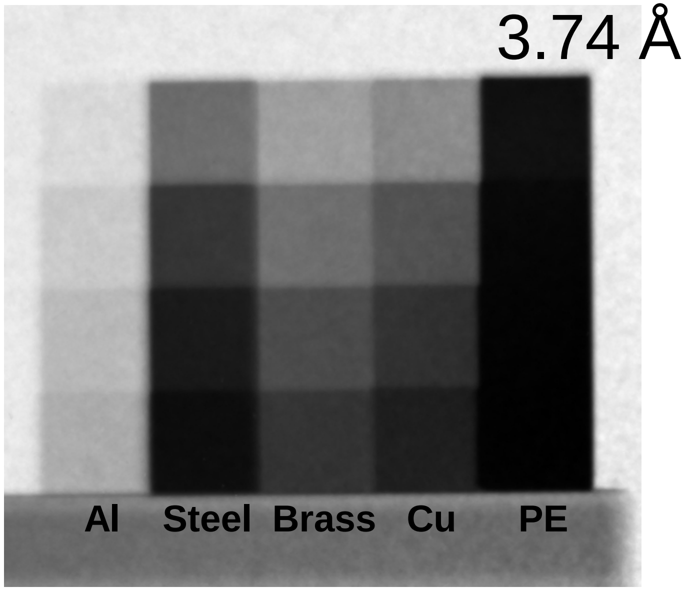
3.74 Å
Al Steel Brass Cu PE

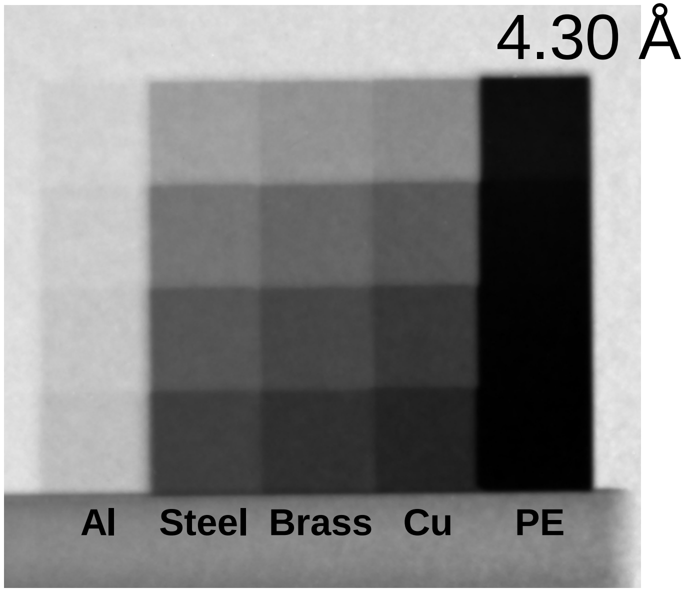
4.30 Å
Al Steel Brass Cu PE

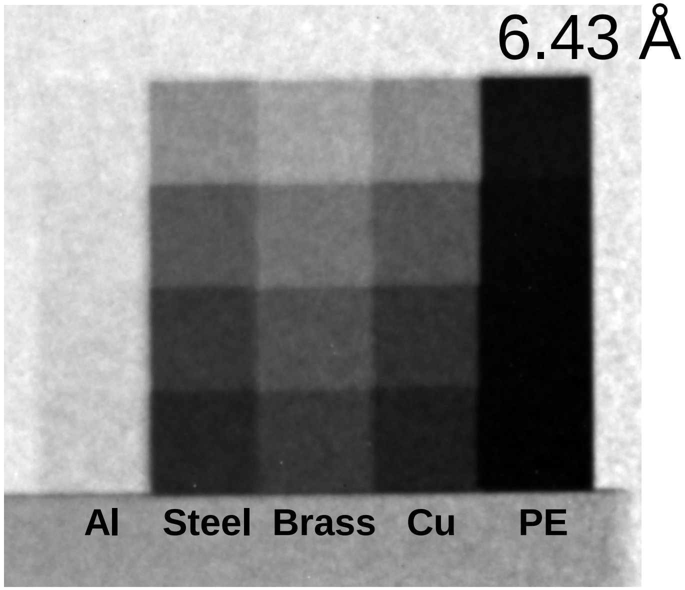
6.43 Å
Al Steel Brass Cu PE

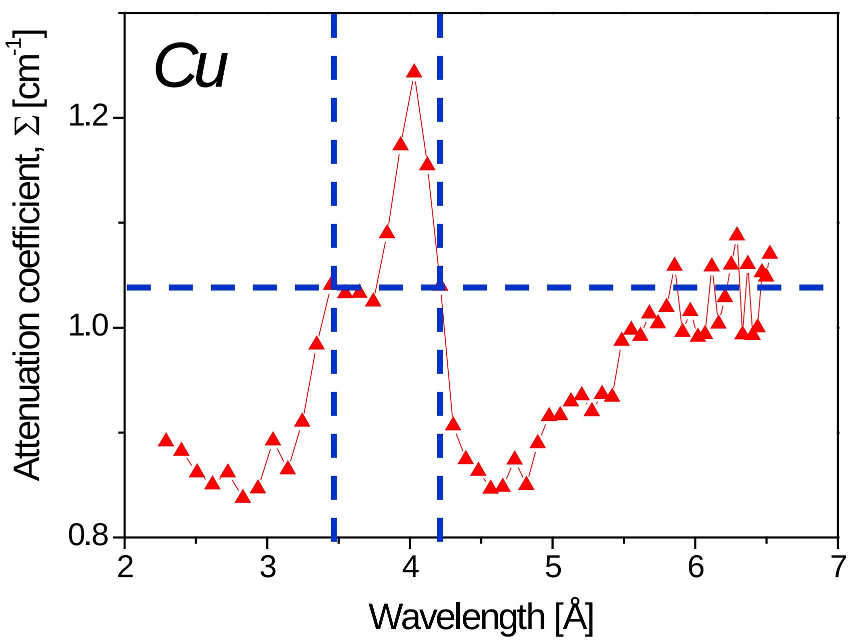
Cu
Attenuation coefficient, Σ [cm^{-1}]
0.8
1.0
1.2
2
3
4
5
6
7
Wavelength [Å]

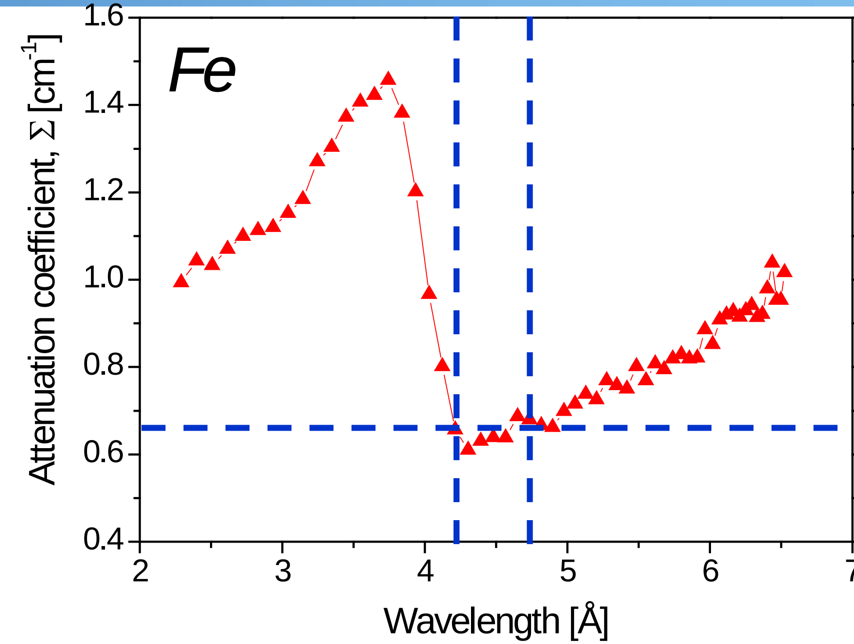
Fe
Attenuation coefficient, Σ [cm^{-1}]
0.4
0.6
0.8
1.0
1.2
1.4
1.6
2
3
4
5
6
7
Wavelength [Å]

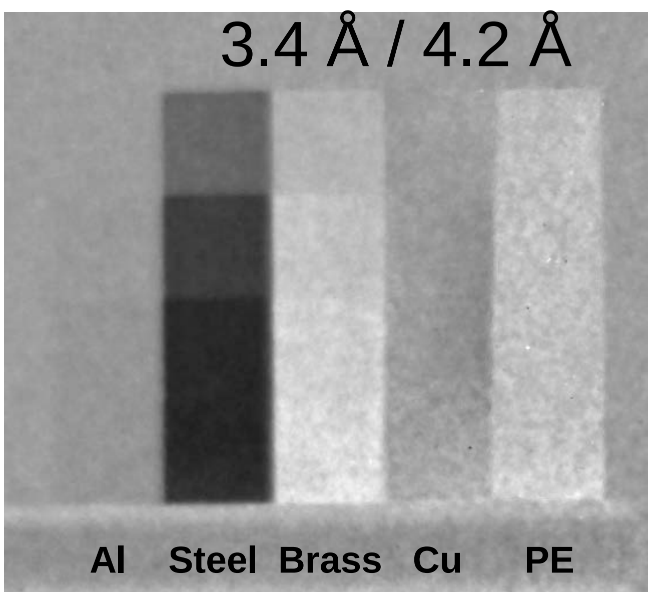
3.4 Å / 4.2 Å
Al
Steel
Brass
Cu
PE

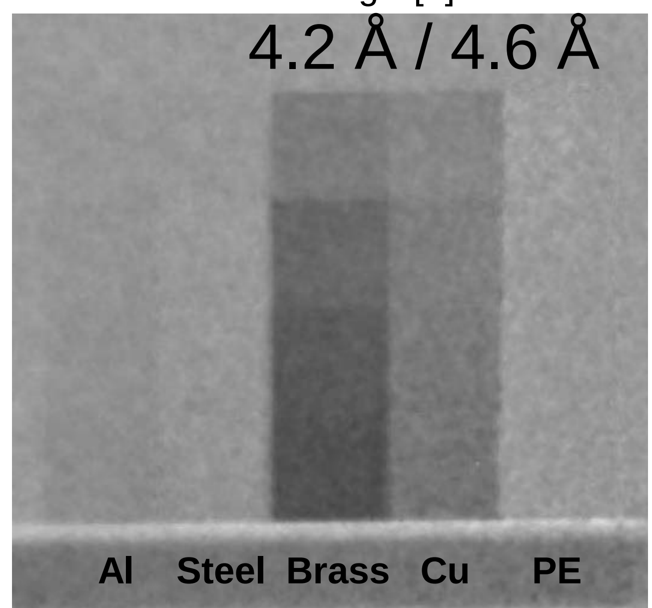
4.2 Å / 4.6 Å
Al
Steel
Brass
Cu
PE

Energy-selective radiography

Weld (photo)

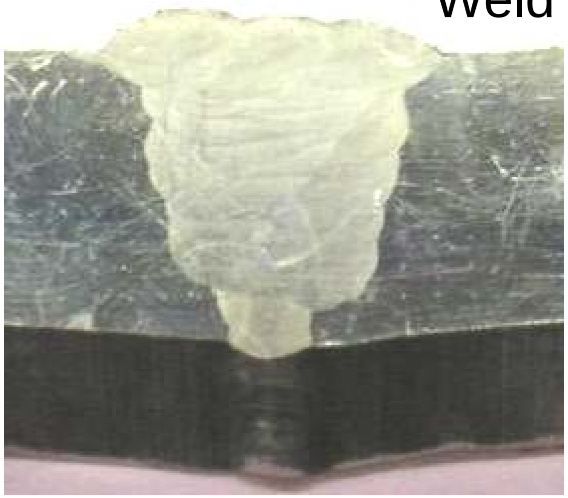

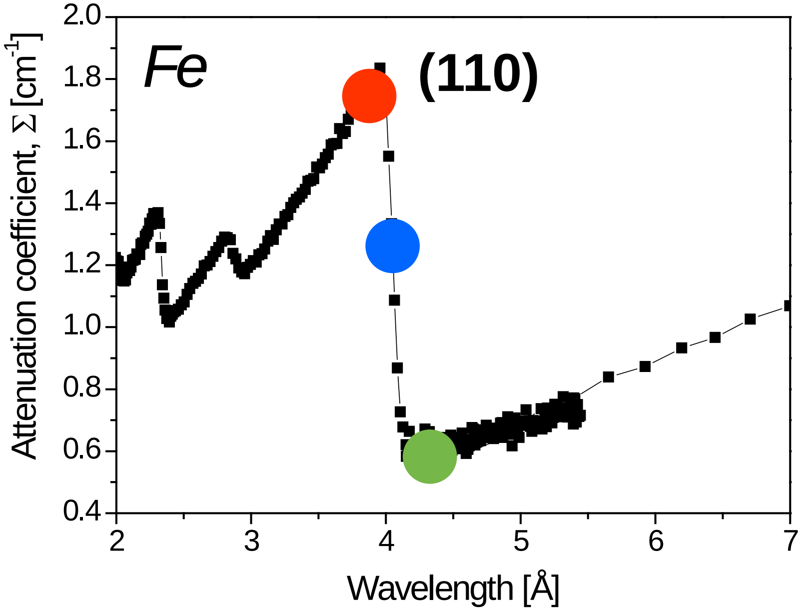

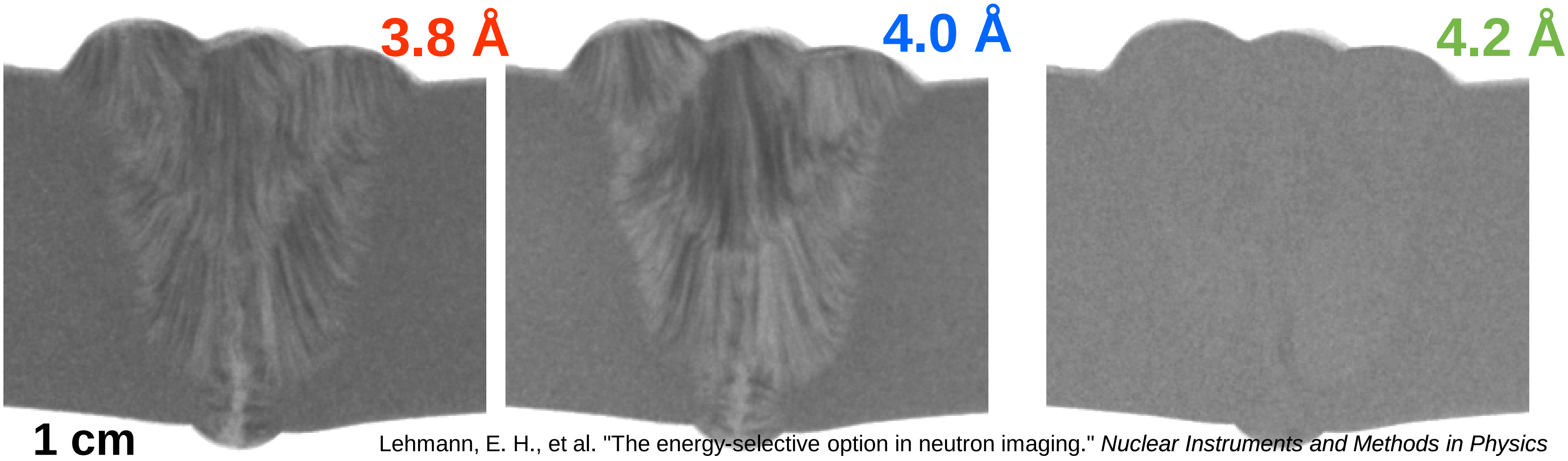

Lehmann, E. H., et al. "The energy-selective option in neutron imaging." *Nuclear Instruments and Methods in Physics Research Section A: Accelerators, Spectrometers, Detectors and Associated Equipment* 603.3 (2009): 429-438.

Diffraction Contrast

Mesopotamian Seals (from c. 2000 - 1600 BC)

(Theo Krispijn, *NINO Institute*, Dirk Visser, *Delft University of Techn*ology, Holland)

Photo

Neutron radiography

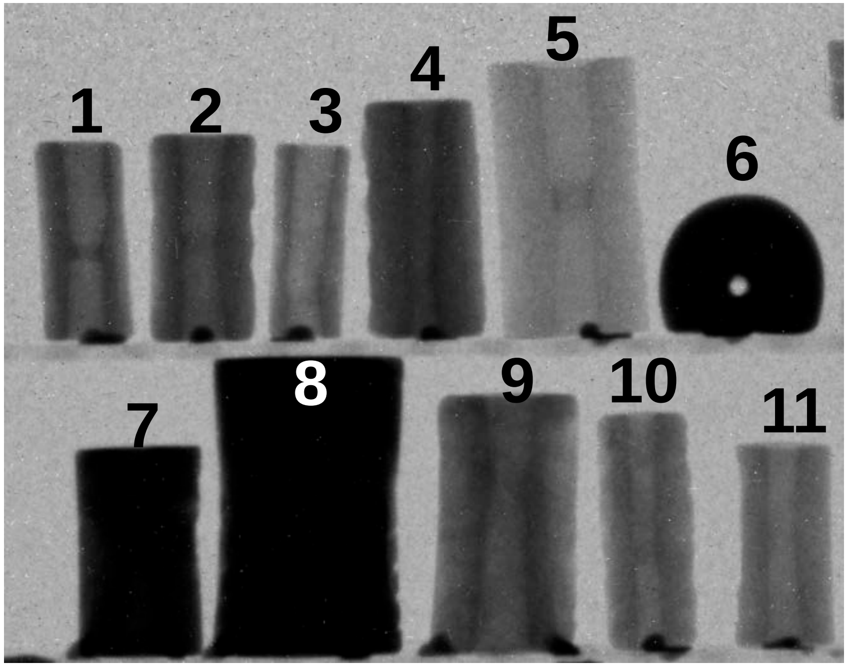

1 cm

The De Liagre-Böhl collection of the Dutch Institute for the Near East (NINO) houses about 150 seals, 13 of which were visually identified as hematite. The seals were acquired in Iraq at the beginning of the last century.

Diffraction Contrast

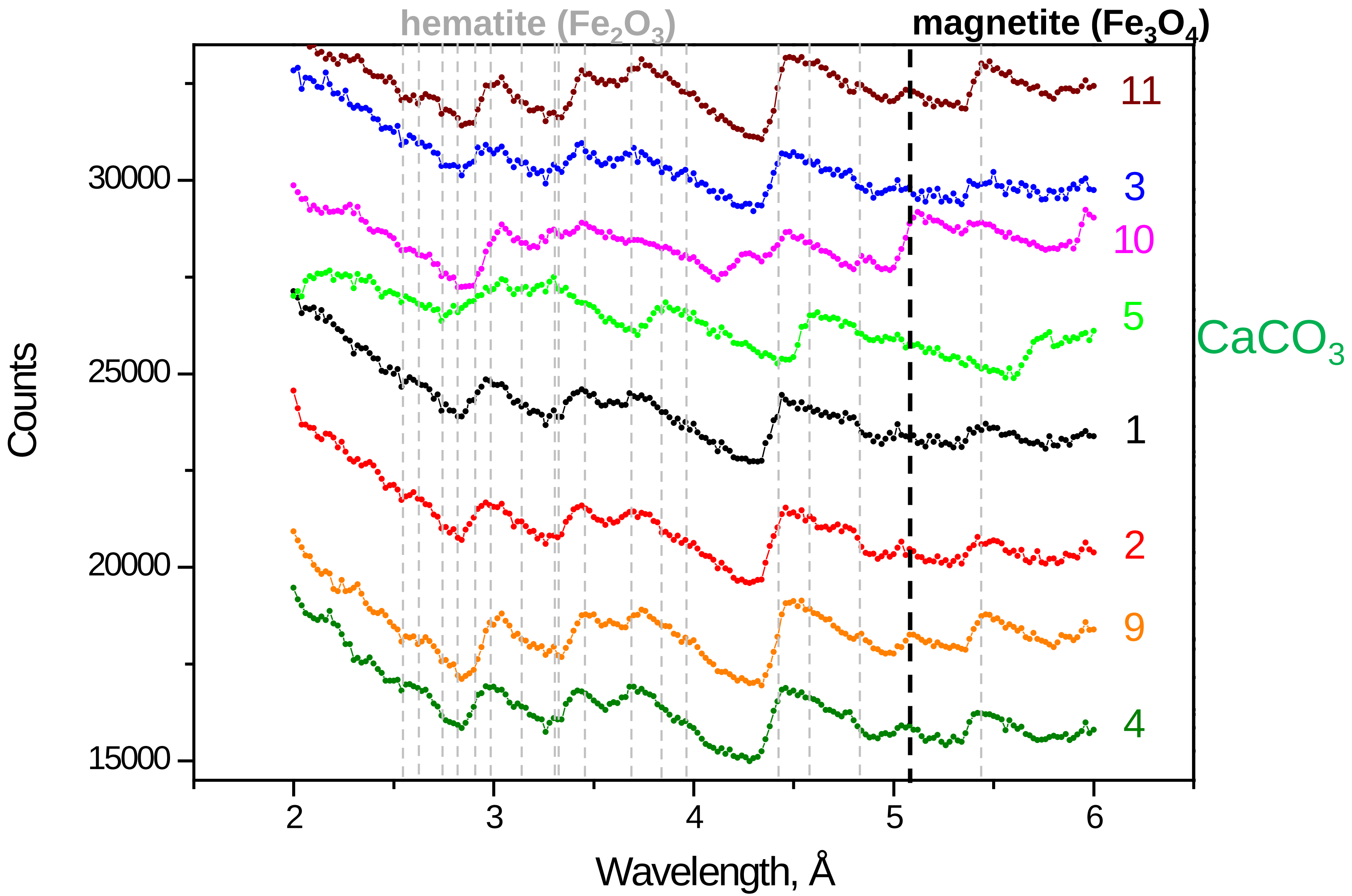

Diffraction Contrast

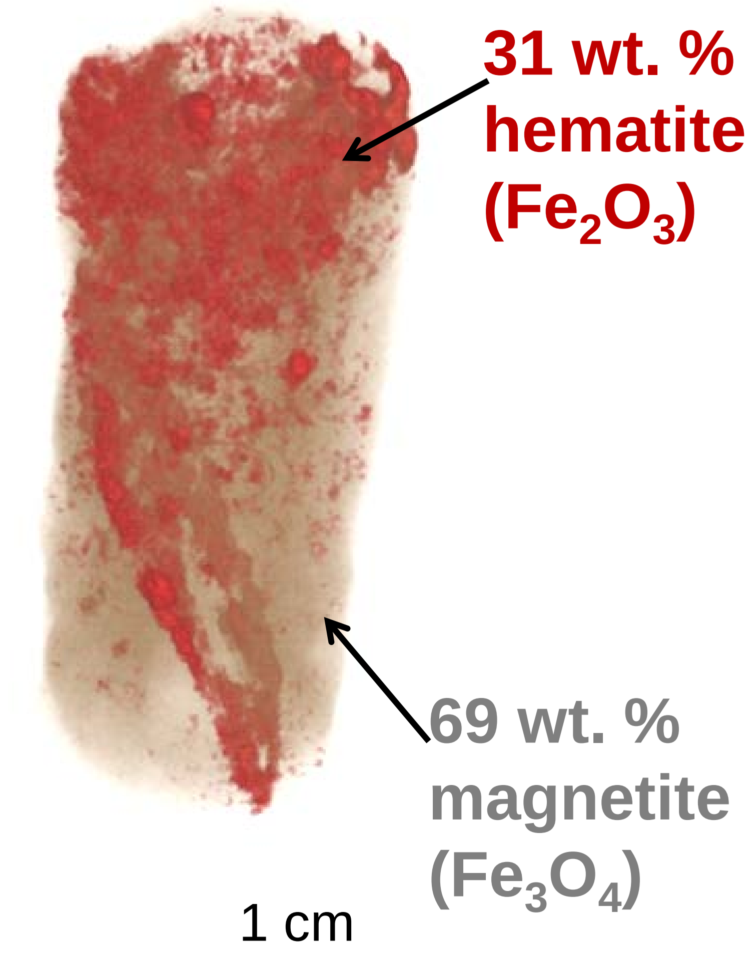

3D Phase mapping in metals

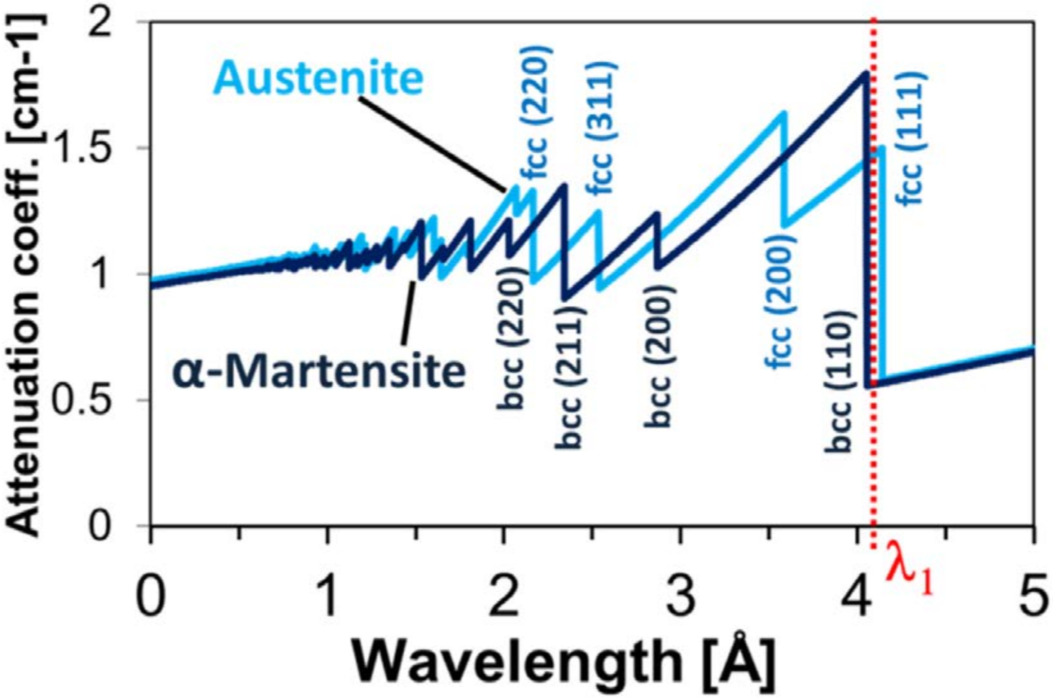

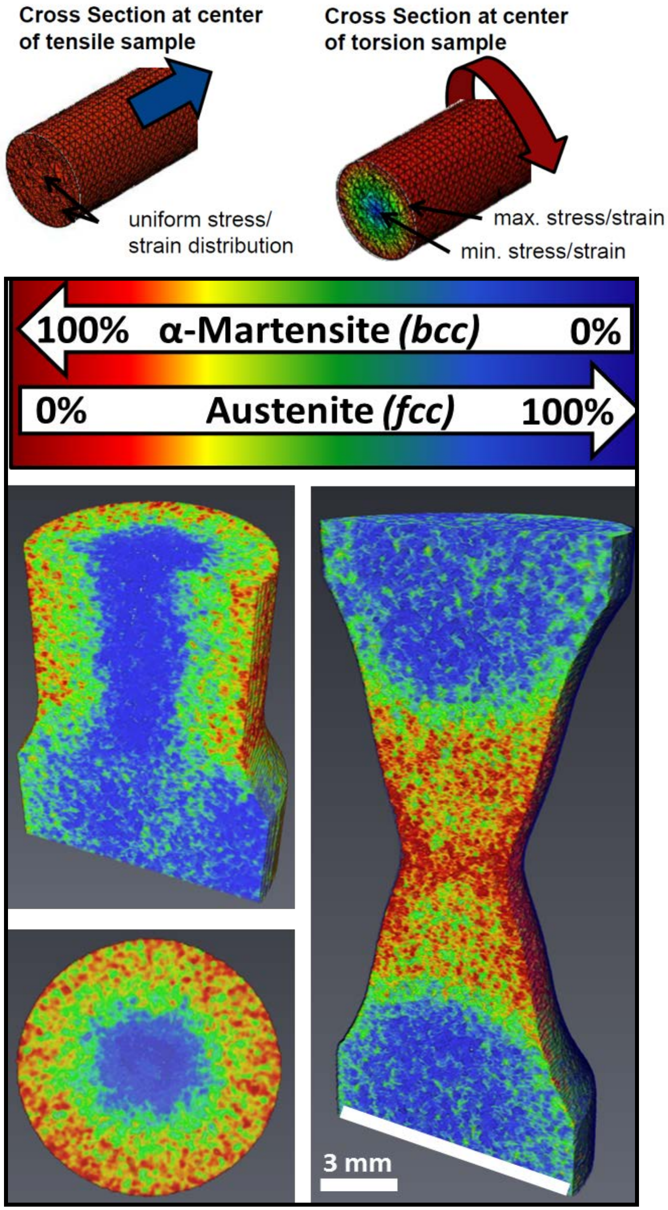

Energy-selective neutron tomography of TRIP-steel

R. Woracek et al., **Advanced Materials**, in print (2014)

Residual stresses

(Dayakar Penumadu, Robin Woracek, *University of Tennessee*, Knoxville, USA)

Setup for energy selective imaging

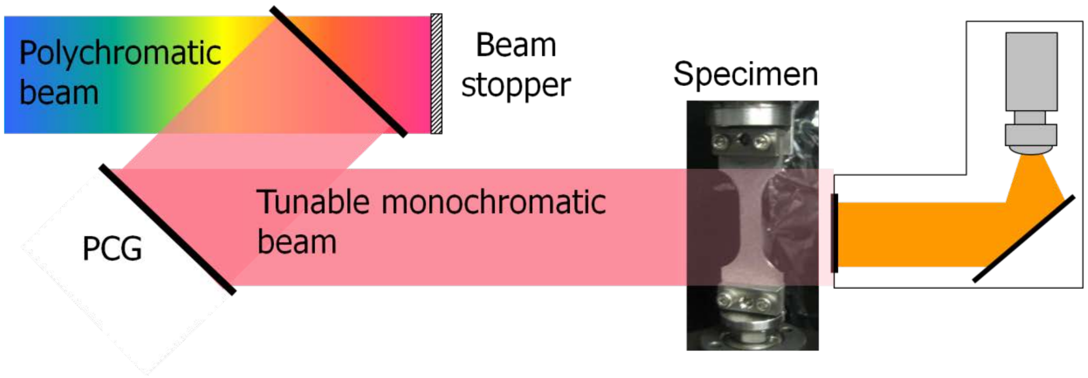

Multi-Axial Loading System

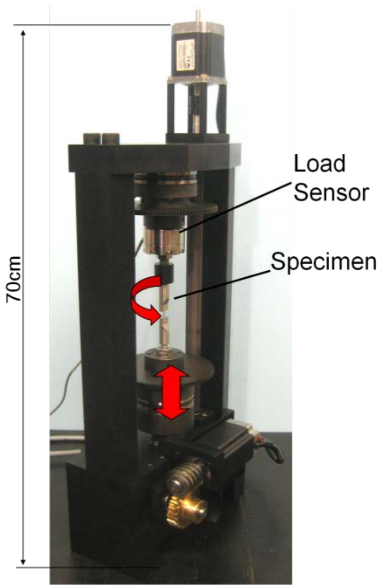

Diffraction Contrast

Residual stresses

(Dayakar Penumadu, Robin Voracek, *University of Tennessee*, Knoxville, USA)

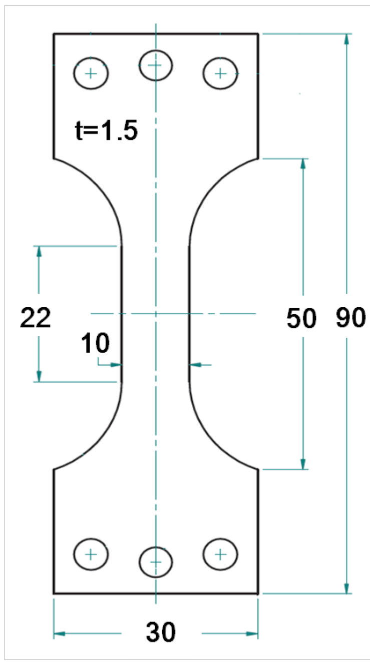

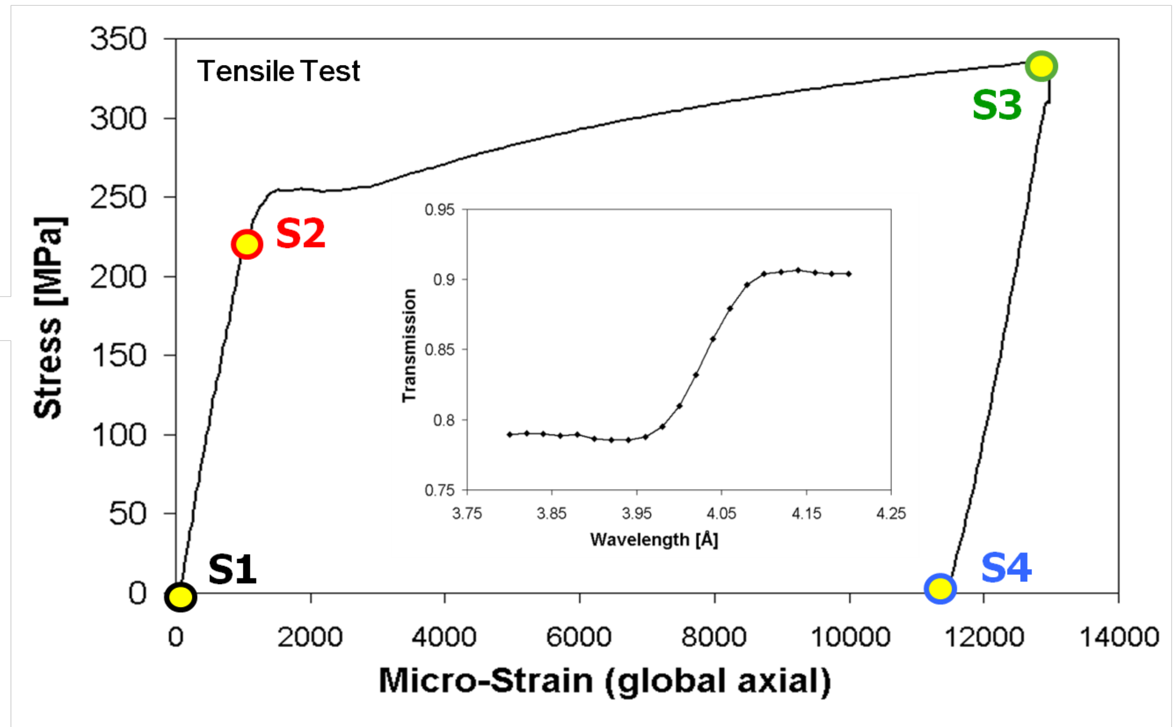

Insert: [110] Bragg Edge for point S1. The position of the Bragg Edge was obtained by fitting using Gauss's non-linear least-squares method.

Diffraction Contrast

Residual stresses

(Dayakar Penumadu, Robin Voracek, *University of Tennessee*, Knoxville, USA)

Imaging measurements

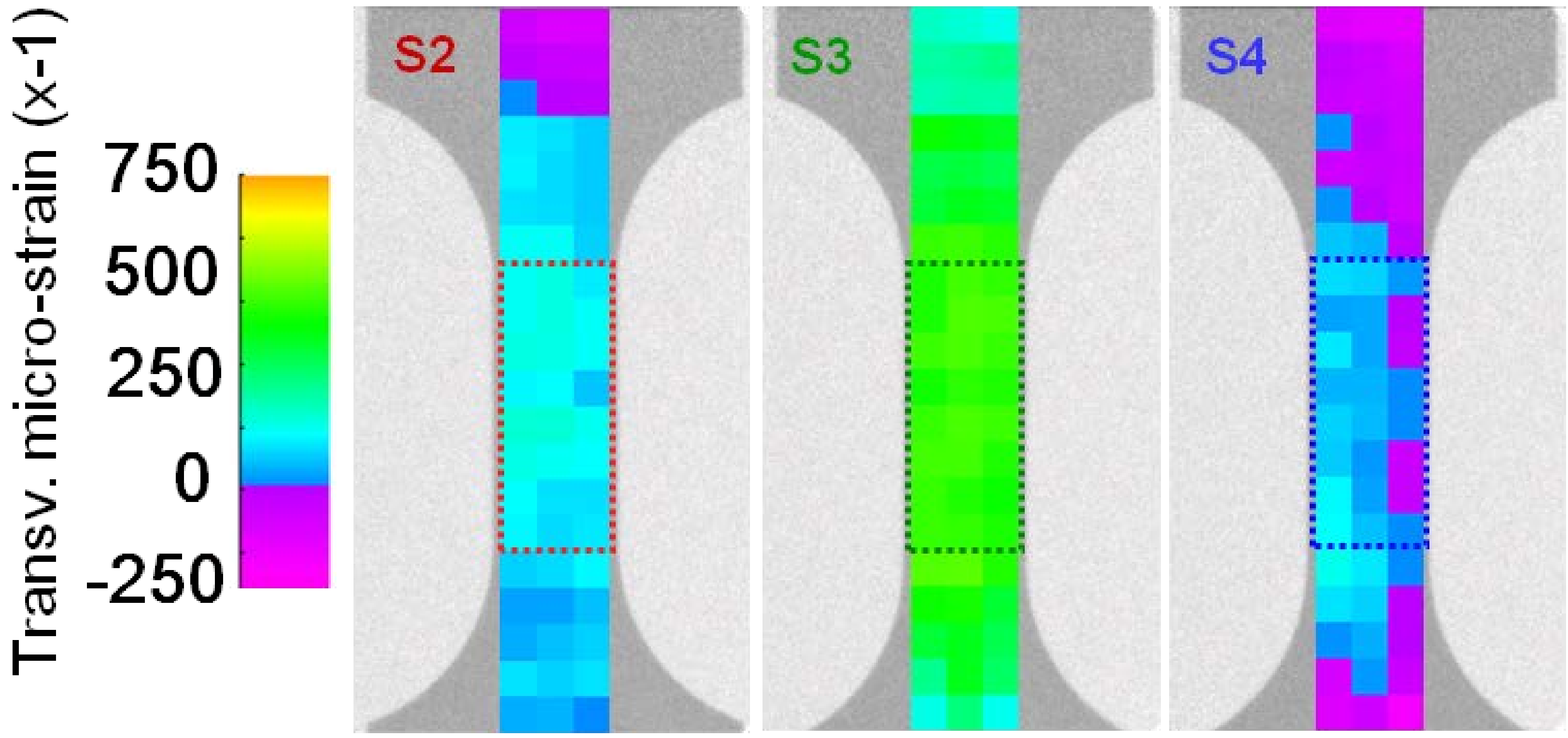

Residual stresses

(Robin Woracek, *University of Tennessee*, USA, Robert Wimpory, *HZB*, Germany)

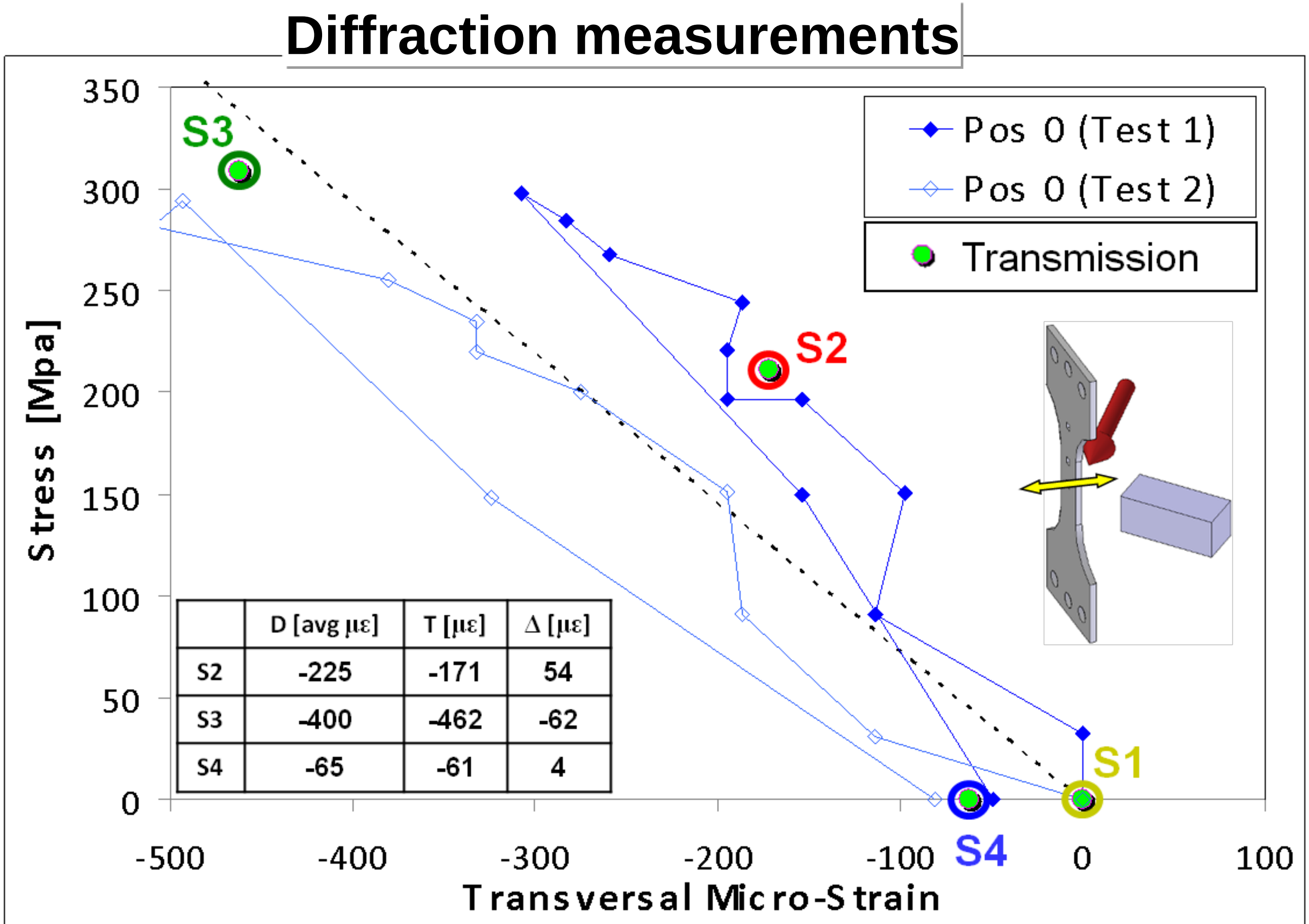

	D [avg με]	T [με]	Δ [με]
S2	-225	-171	54
S3	-400	-462	-62
S4	-65	-61	4

Phase/Dark-field Contrast

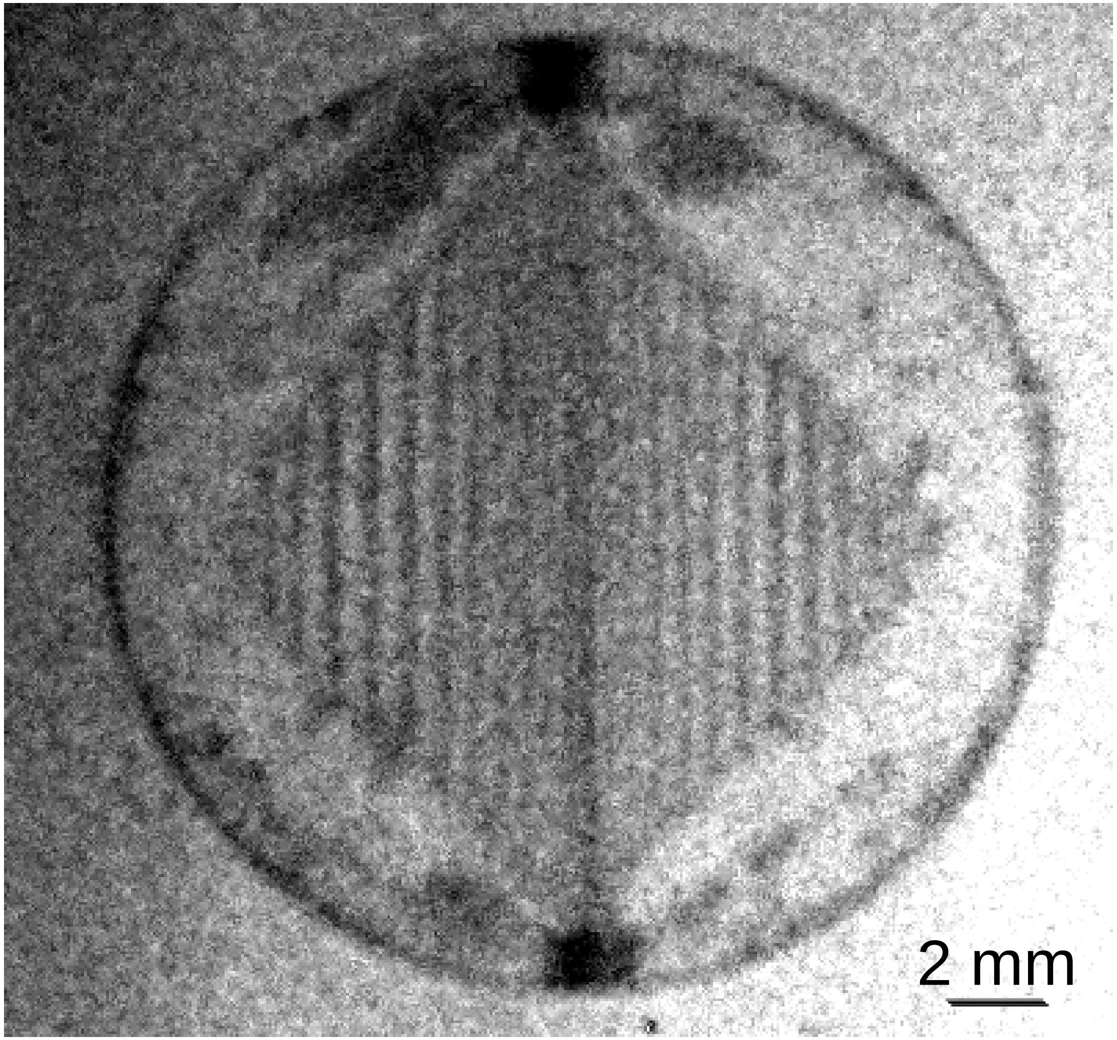

Refractive index:

phase / absorption

$$n(x, y, z, \lambda) = 1 - \delta(x, y, z, \lambda) - i\beta(x, y, z, \lambda)$$

$$\varphi = -k \int_{-\infty}^{z} \delta(z')dz$$

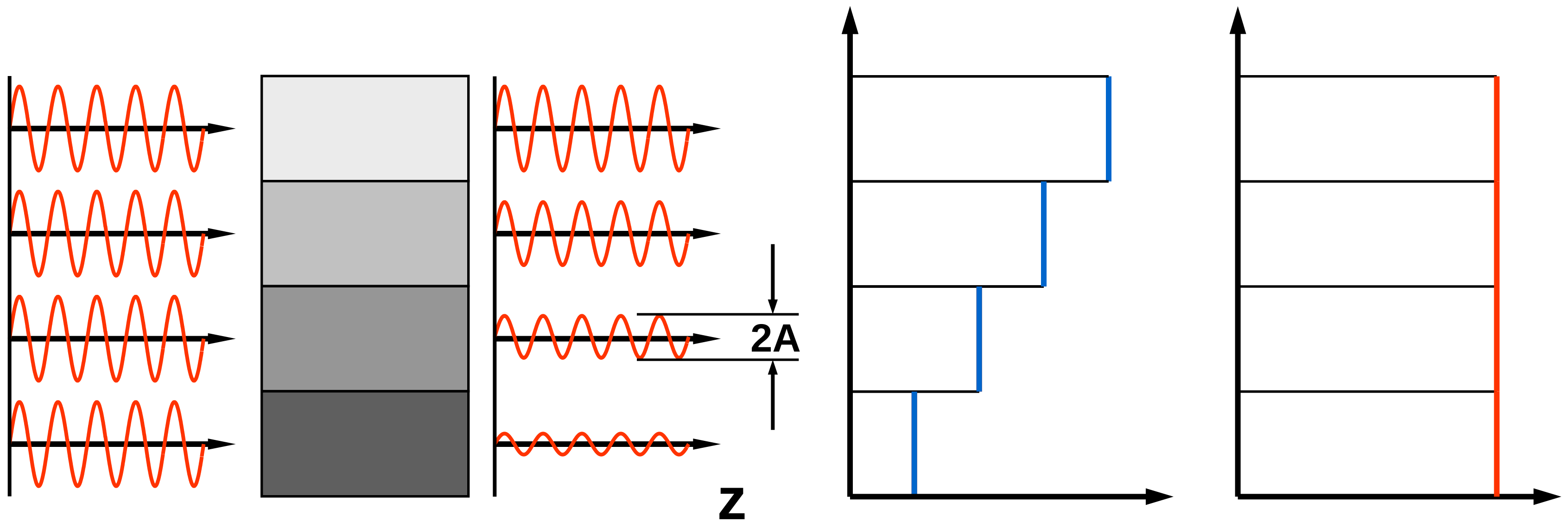

Object
Areas of different transmission

Absorption-contrast

Phase-contrast

Introduction

Refractive index:

$$n(x, y, z, \lambda) = 1 - \underbrace{\delta(x, y, z, \lambda)}_{\text{phase}} - i\underbrace{\beta(x, y, z, \lambda)}_{\text{absorption}}$$

$$\varphi = -k \int_{-\infty}^{z} \delta(z')dz$$

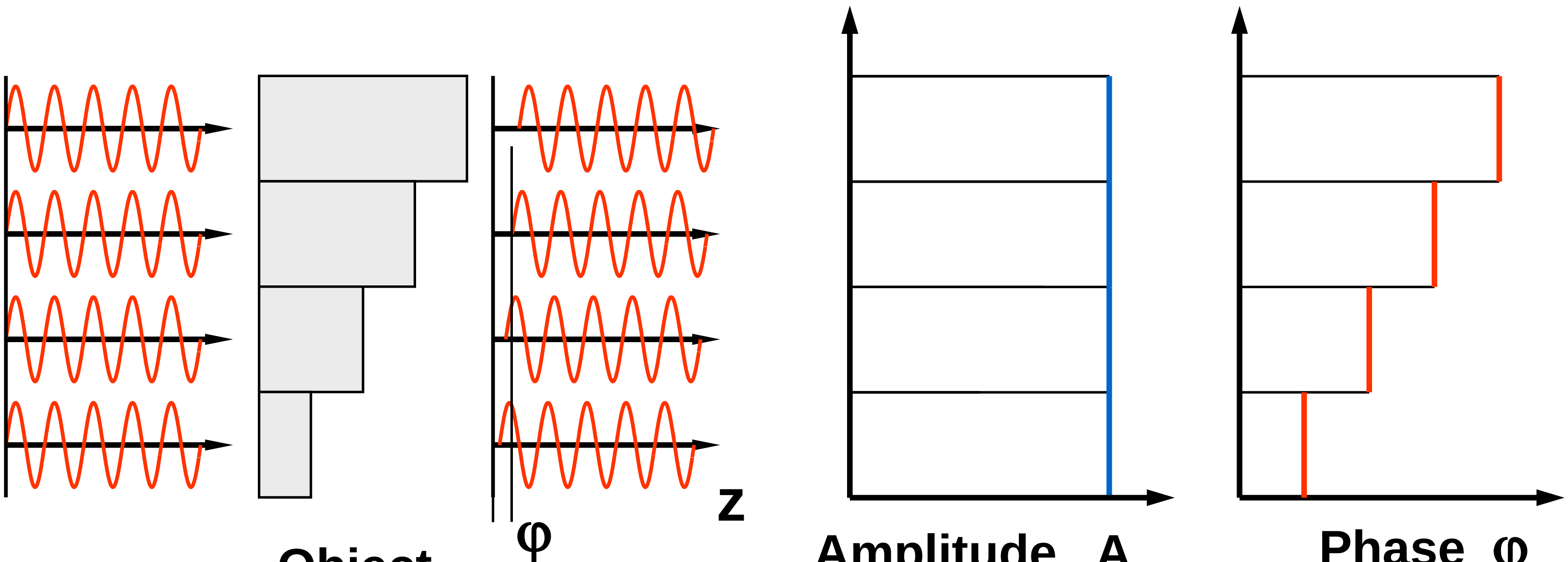

Object
Areas of different thickness/phase shifts

Amplitude A

Absorption-contrast

Phase φ

Phase-contrast

Phase contrast imaging based on Fresnel propagation

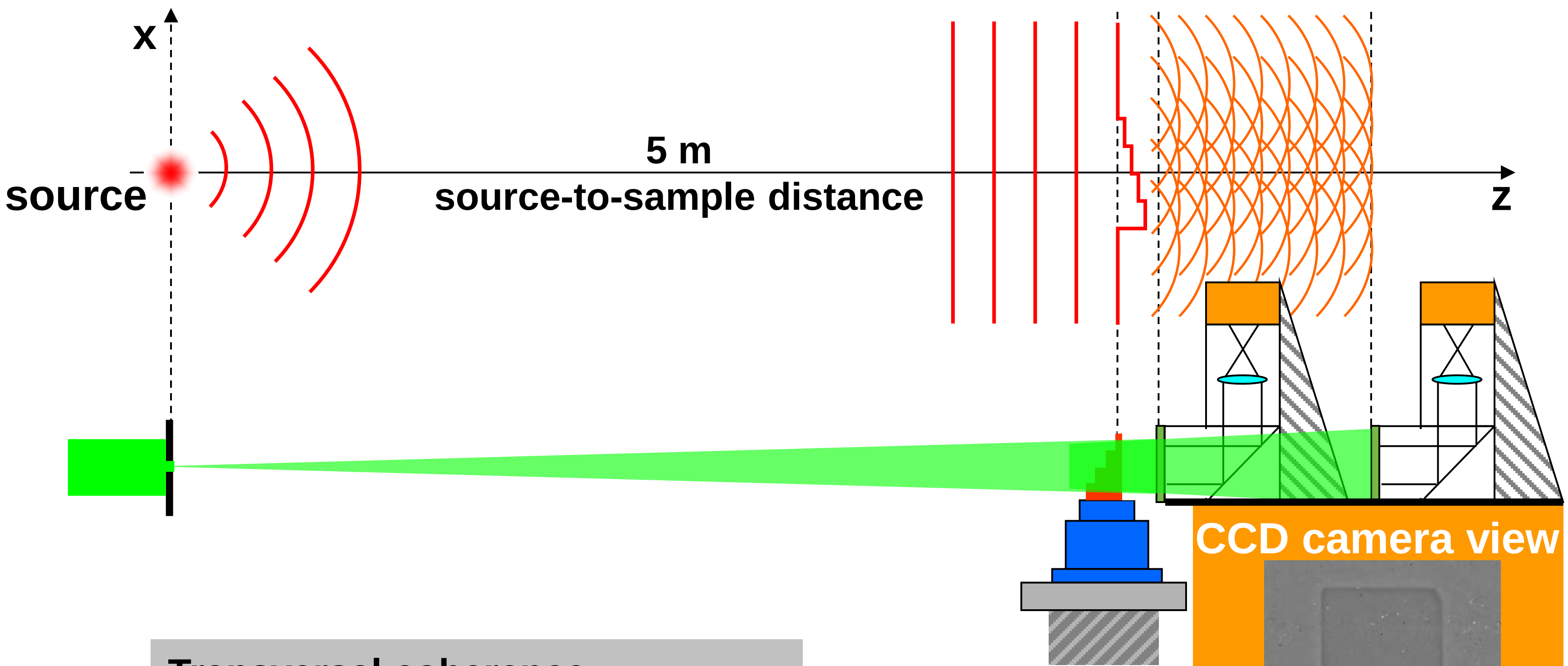

Transversal coherence

l **≤ L λ / s**

Example:	**Thermal neutrons**
λ=0.2nm	**Wavelength**
L=5m	**Distance**
s=1mm	**Source size**
⇒ *l* ≤ 1µm	**Coherence length**

Phase contrast imaging based on Fresnel propagation

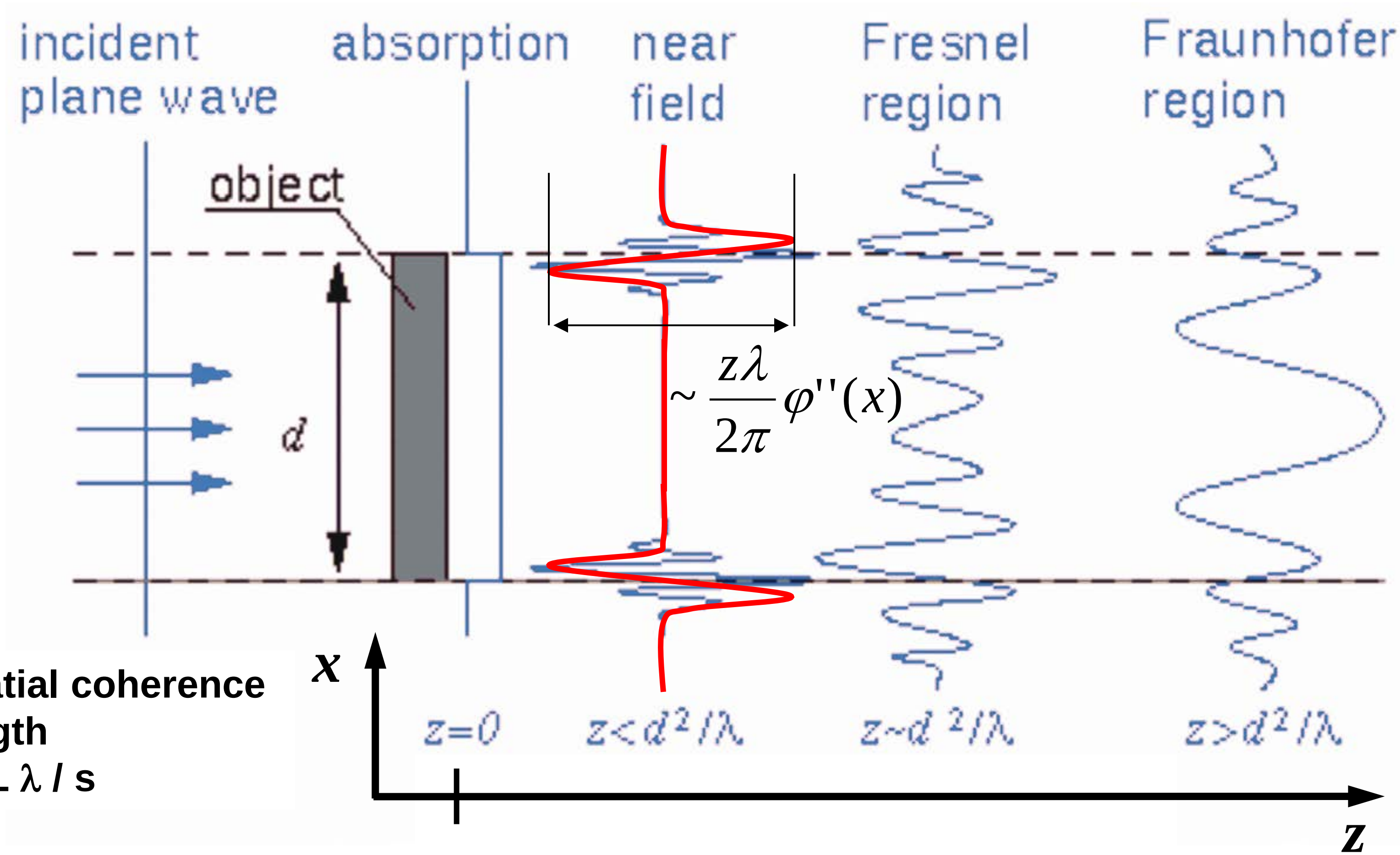

Spatial coherence length
$l \leq L\,\lambda\,/\,s$

Larger λ will improve the spatial coherence of the beam and provide stronger phase-contrast effect.

Phase-contrast pinhole exchanger (5 mm, 3 mm, 1 mm)
Distance pinhole-smaple: ~ 4 m
Distance sample detector: 0 – 700 mm
Polychromatic beam
Transversal coherence length: 0.2 – 1.2 µm (5 mm – 1 mm)

Experimental sketch:

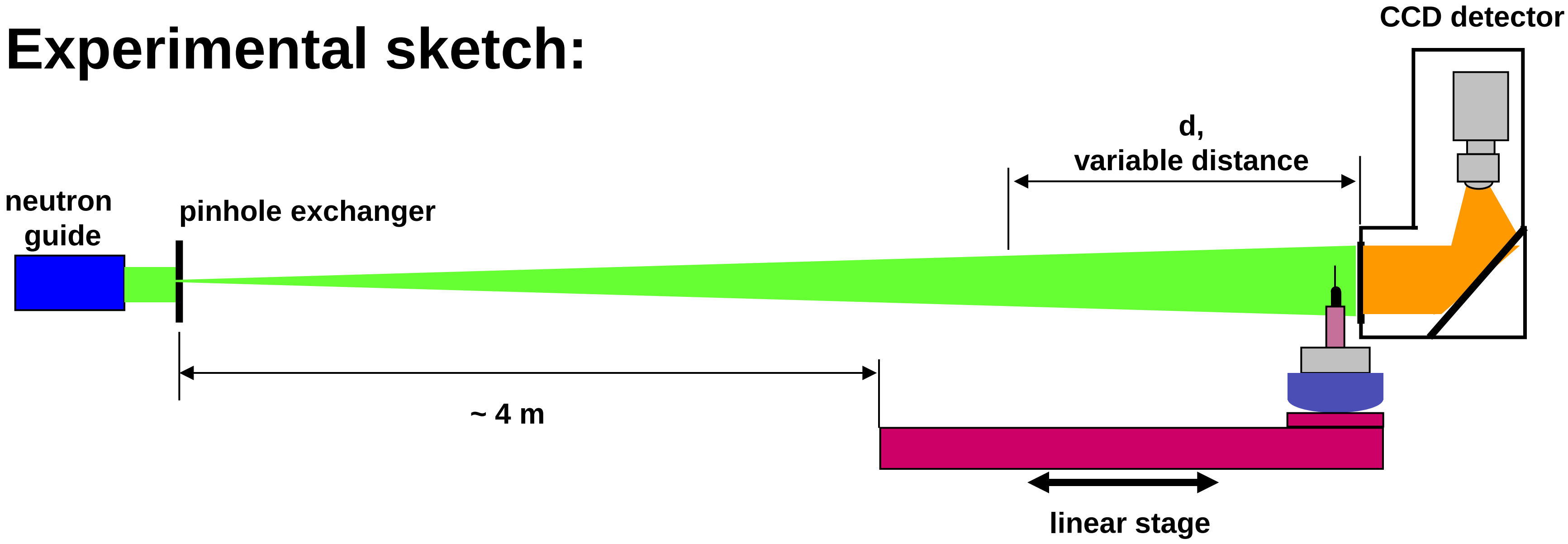

First results

Pinhole 1mm, exp. time 60 min, white beam

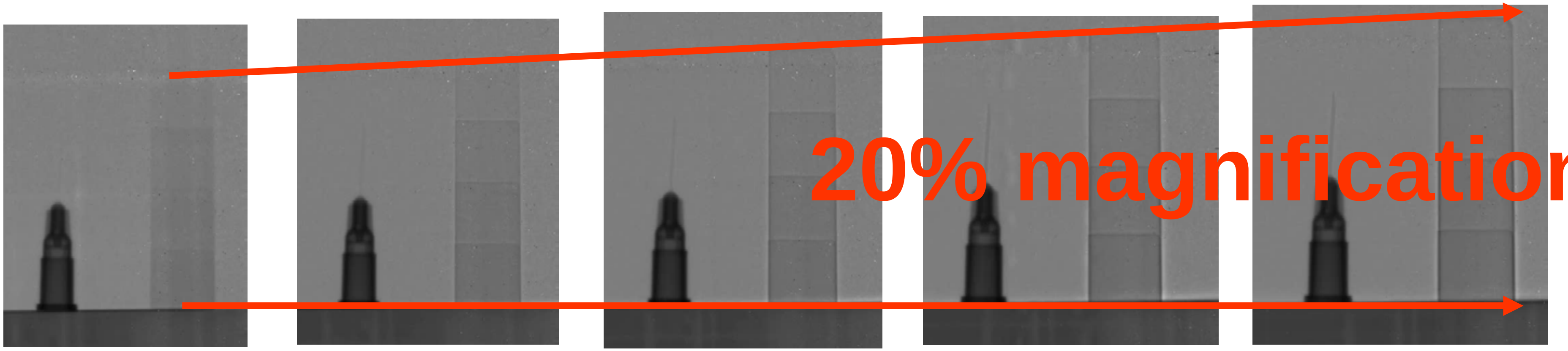

Distance, d: 0 cm **10 cm** **25 cm** **50 cm**

Pinhole 5mm, exp. time 3 min, white beam

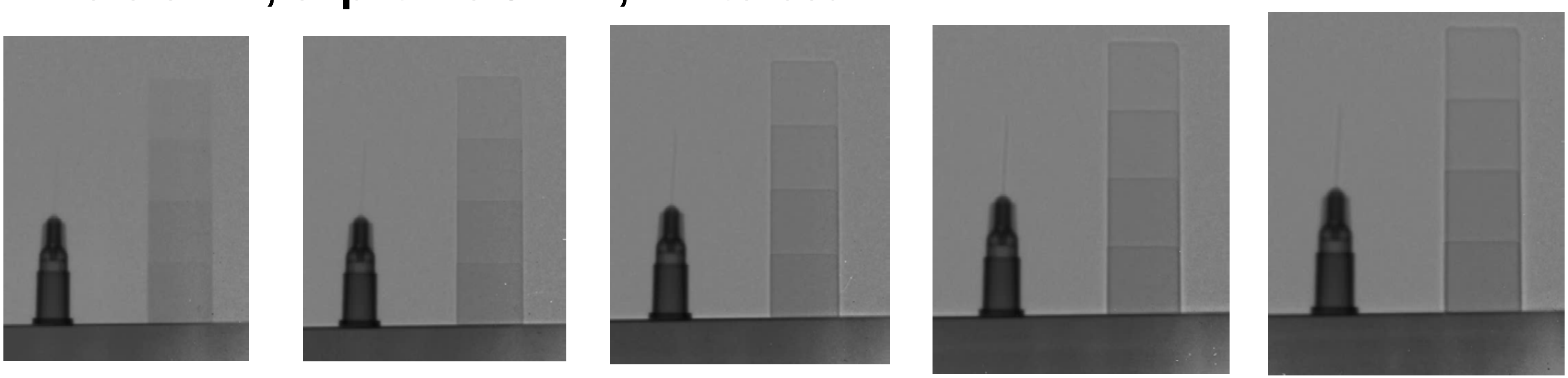

Distance, d: 0 cm **10 cm** **25 cm** **50 cm**

Needle

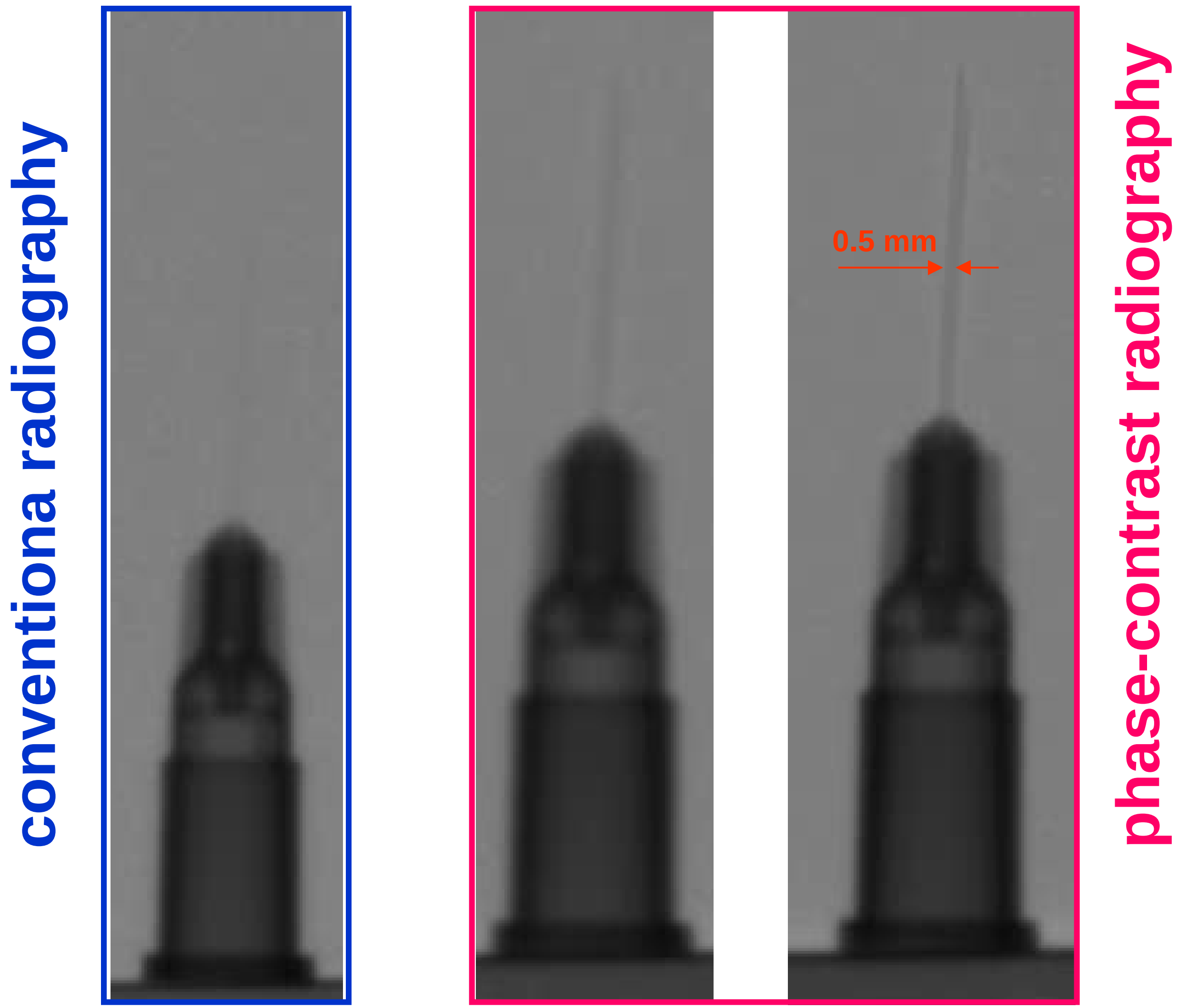

pinhole : 5 mm 5 mm 1 mm
distance : 0 mm 700 mm 700 mm

Al stepwedge

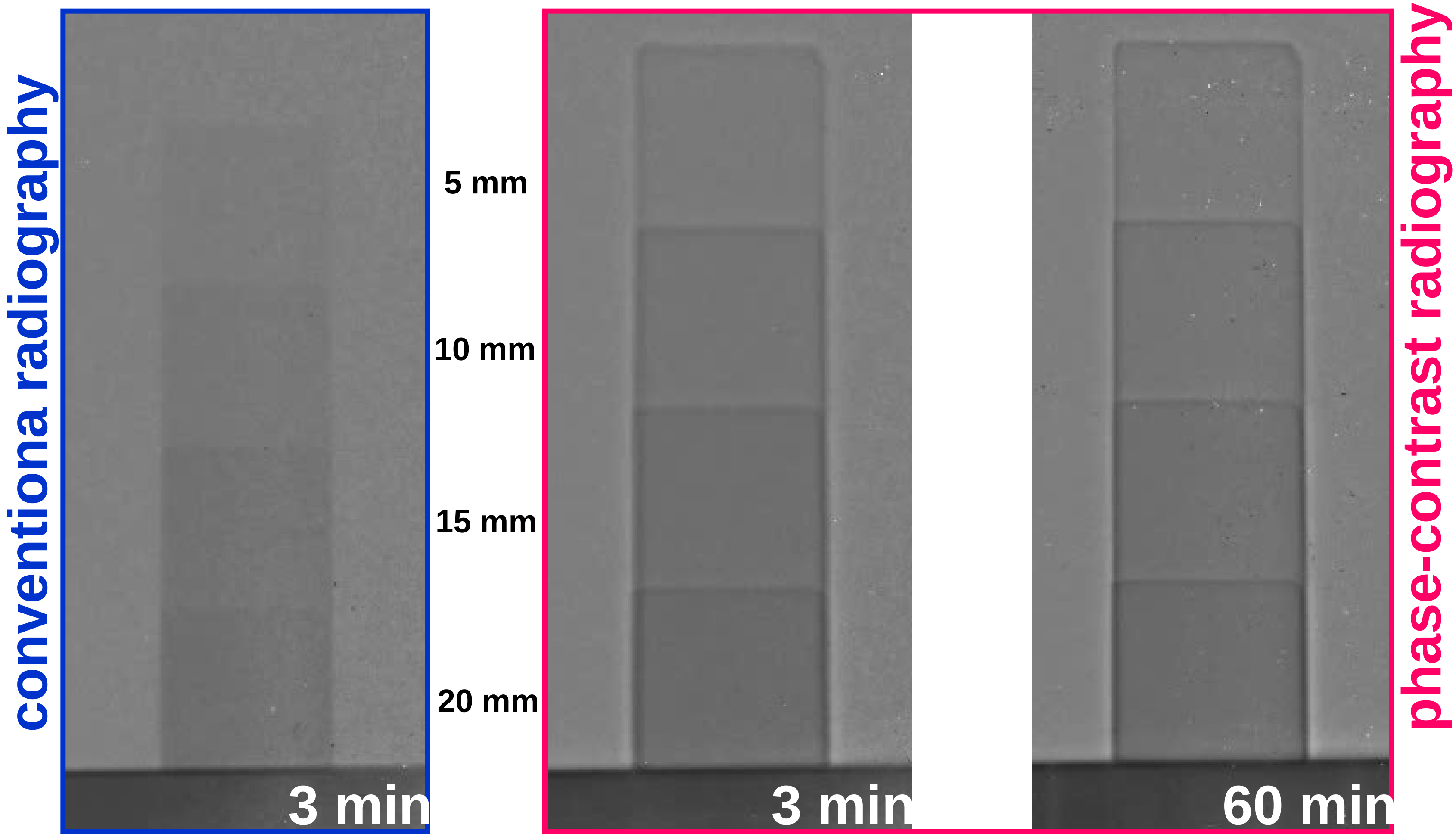

pinhole :	**5 mm**	**5 mm**	**1 mm**
distance :	**0 mm**	**700 mm**	**700 mm**

Refractive index - definition

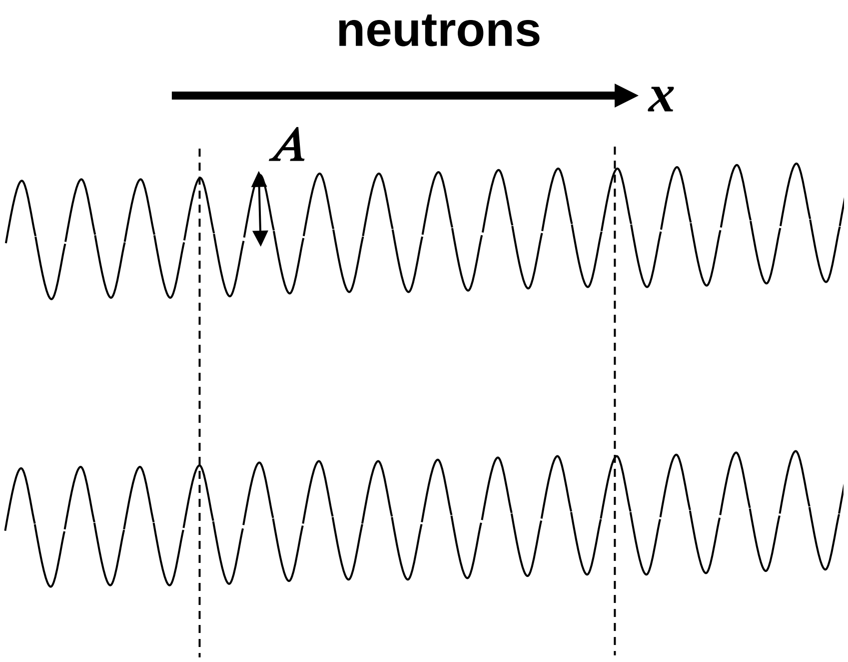

$$\Psi_{before} = A \cdot e^{-i(\omega t - kx)}$$

Refractive index - definition

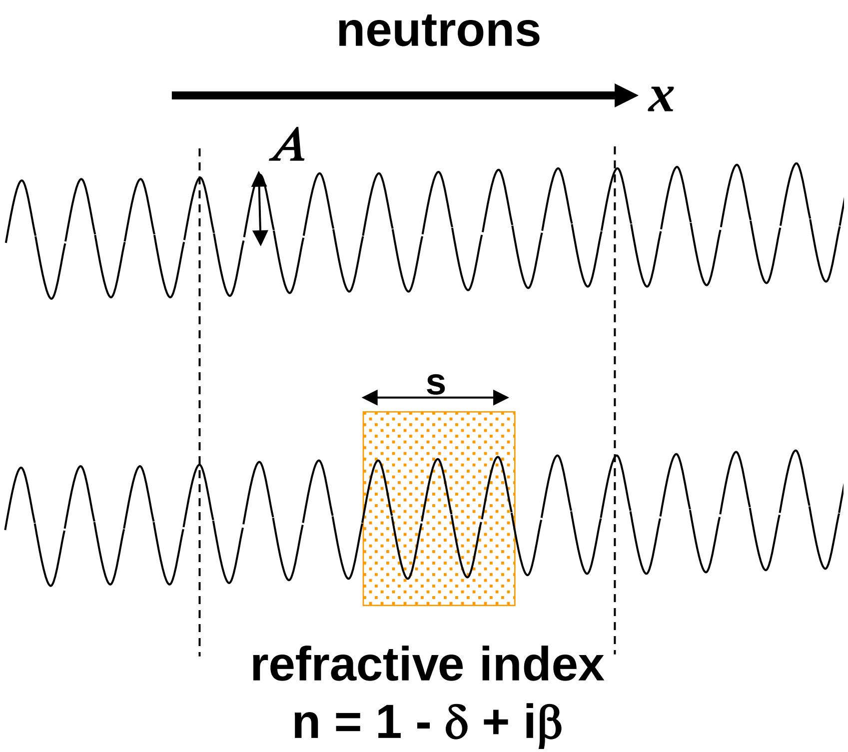

$$\Psi_{before} = A \cdot e^{-i(\omega t - kx)}$$

Refractive index - definition

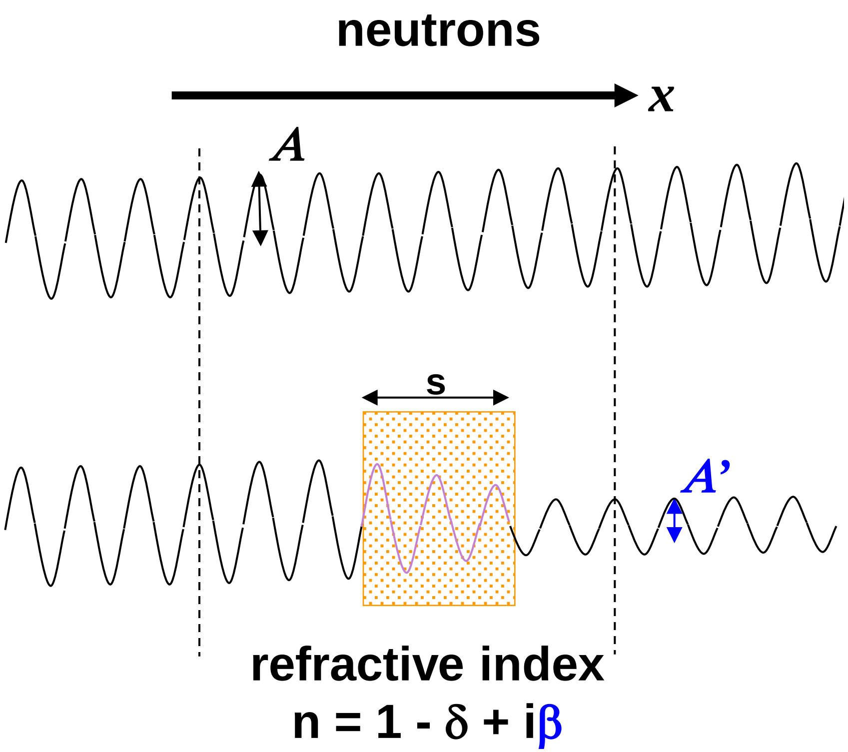

$$\Psi_{before} = A \cdot e^{-i(\omega t - kx)}$$

Refractive index - definition

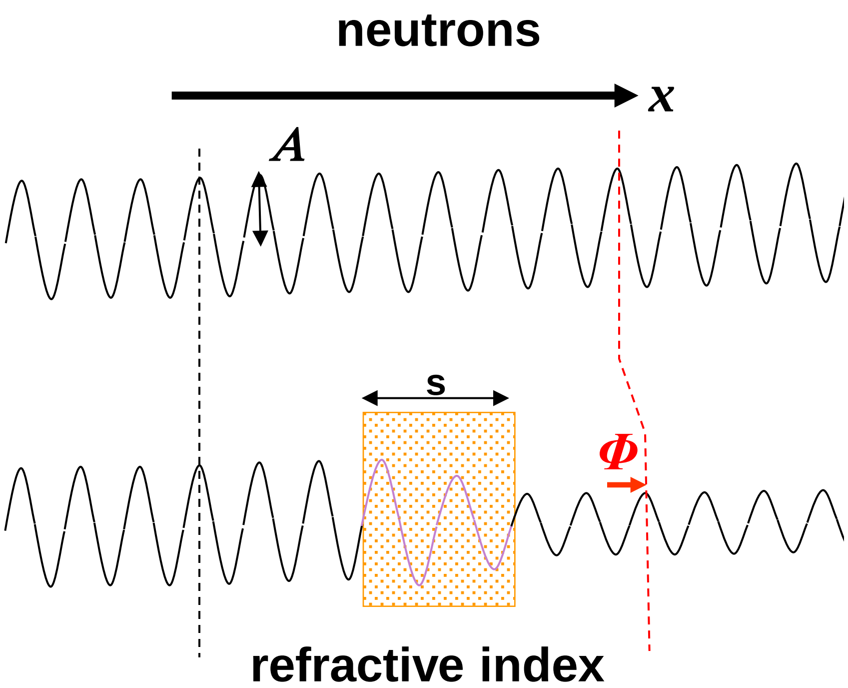

n = 1 - δ + iβ

$$\Psi_{before} = A \cdot e^{-i(\omega t - kx)}$$

Refractive index - definition

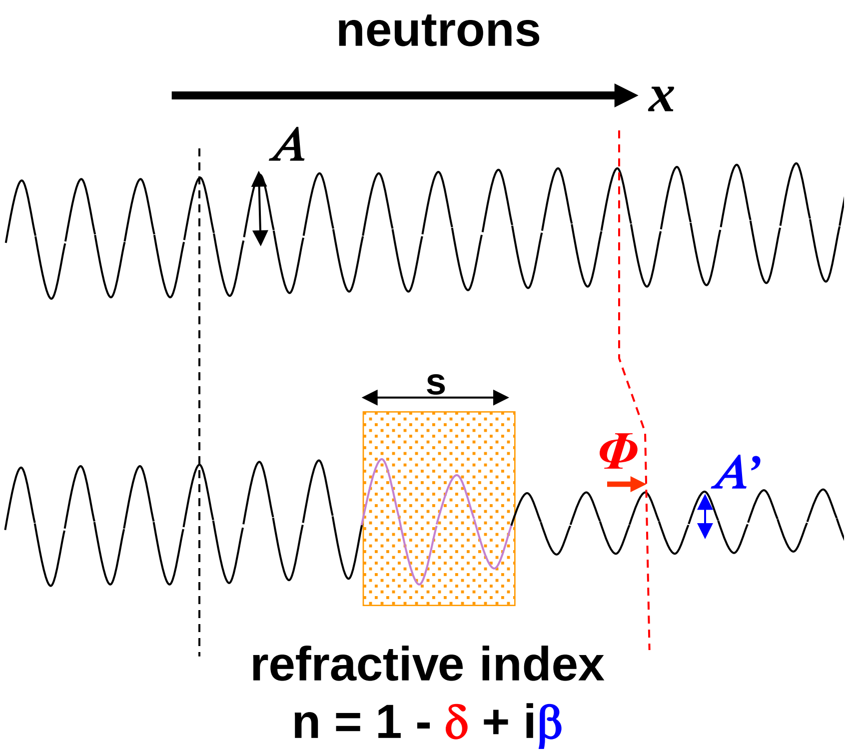

$$\Psi_{before} = A \cdot e^{-i(\omega t - kx)}$$

$$\Psi_{after} = \underbrace{e^{-i(2\pi\delta/\lambda)s}}_{\Phi} \cdot \underbrace{e^{-(2\pi\beta/\lambda)s}}_{A'/A} \cdot \Psi_{before}$$

Grating interferometer

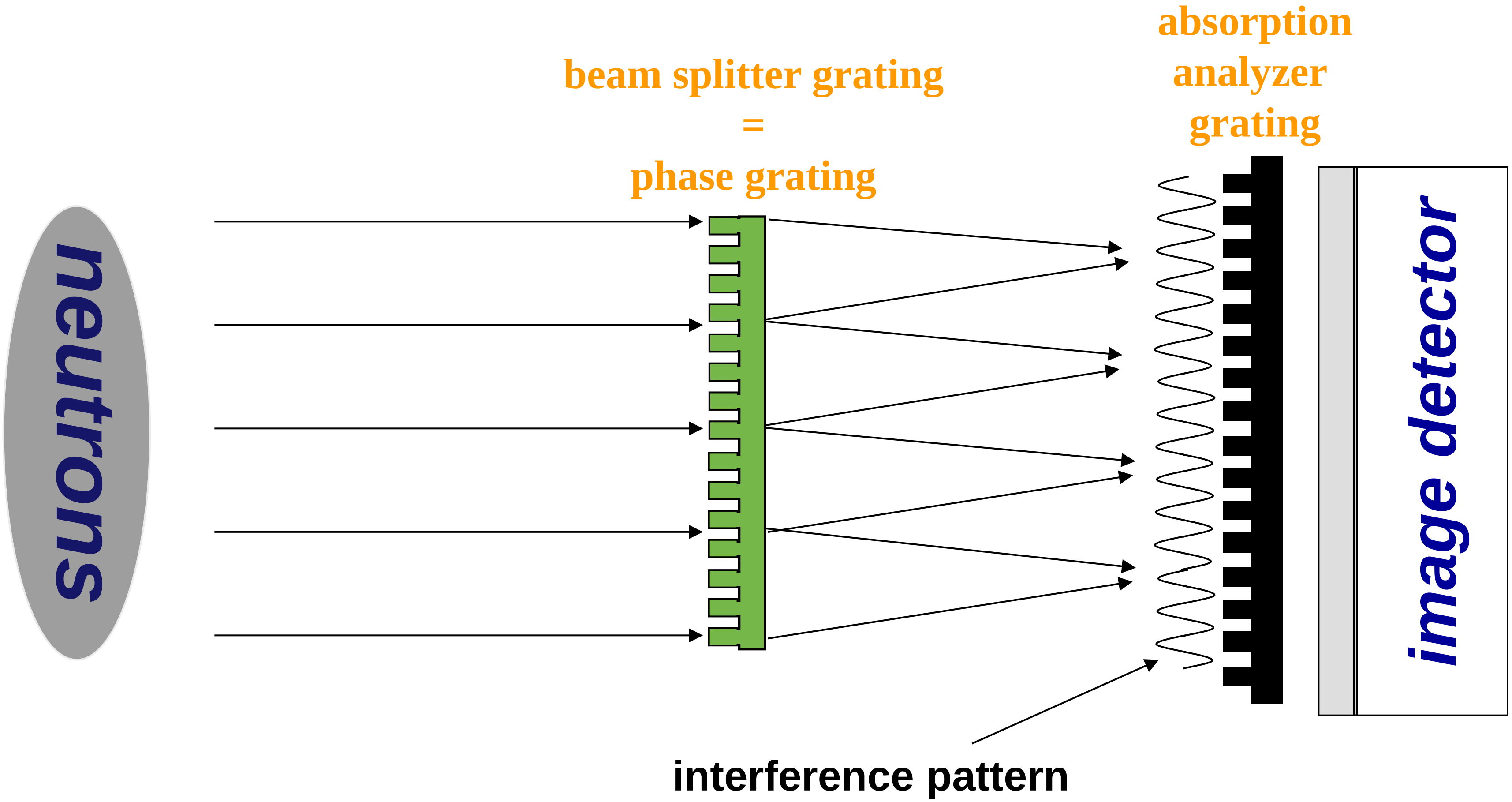

Grating interferometer

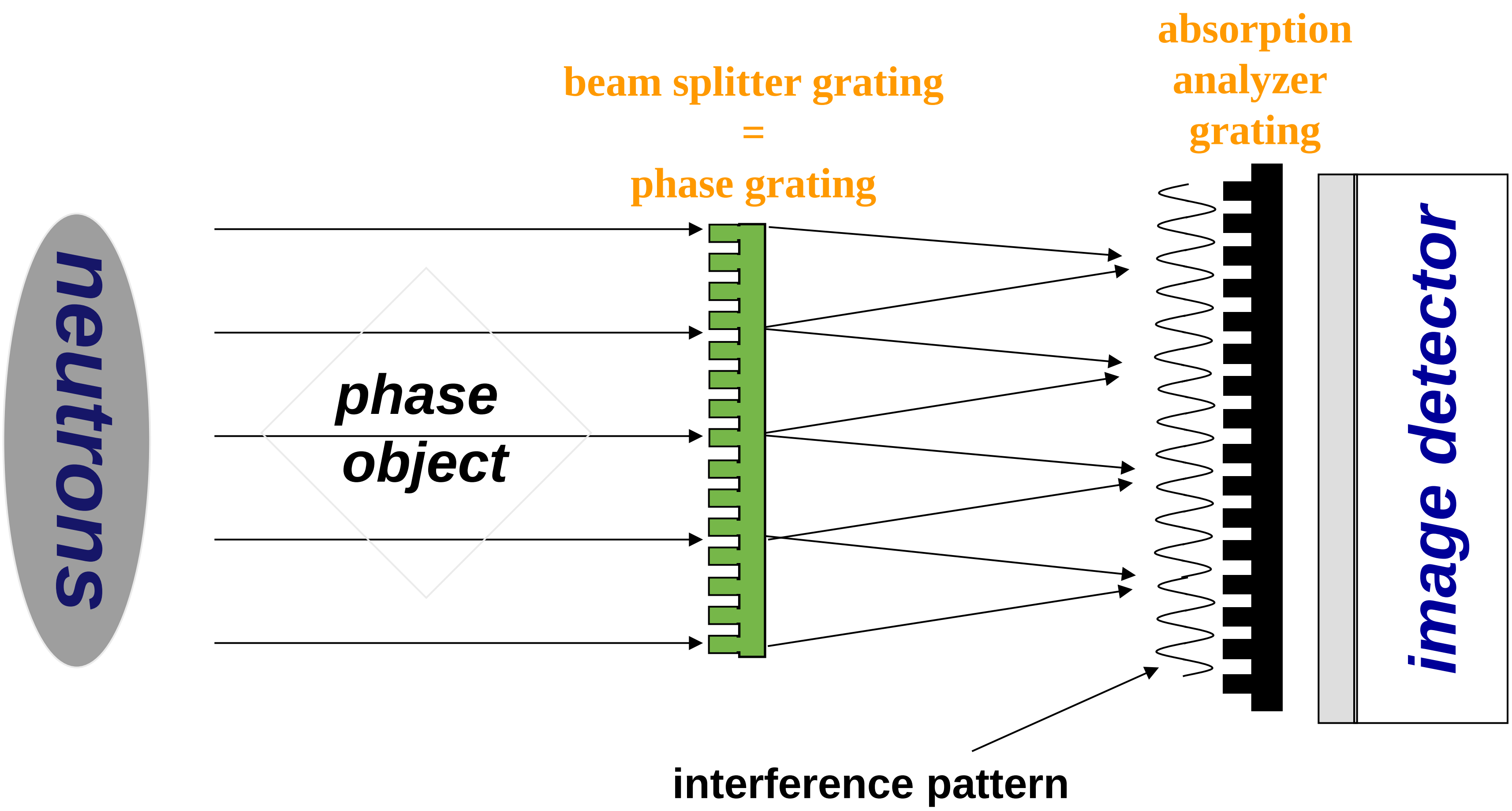

Grating interferometer

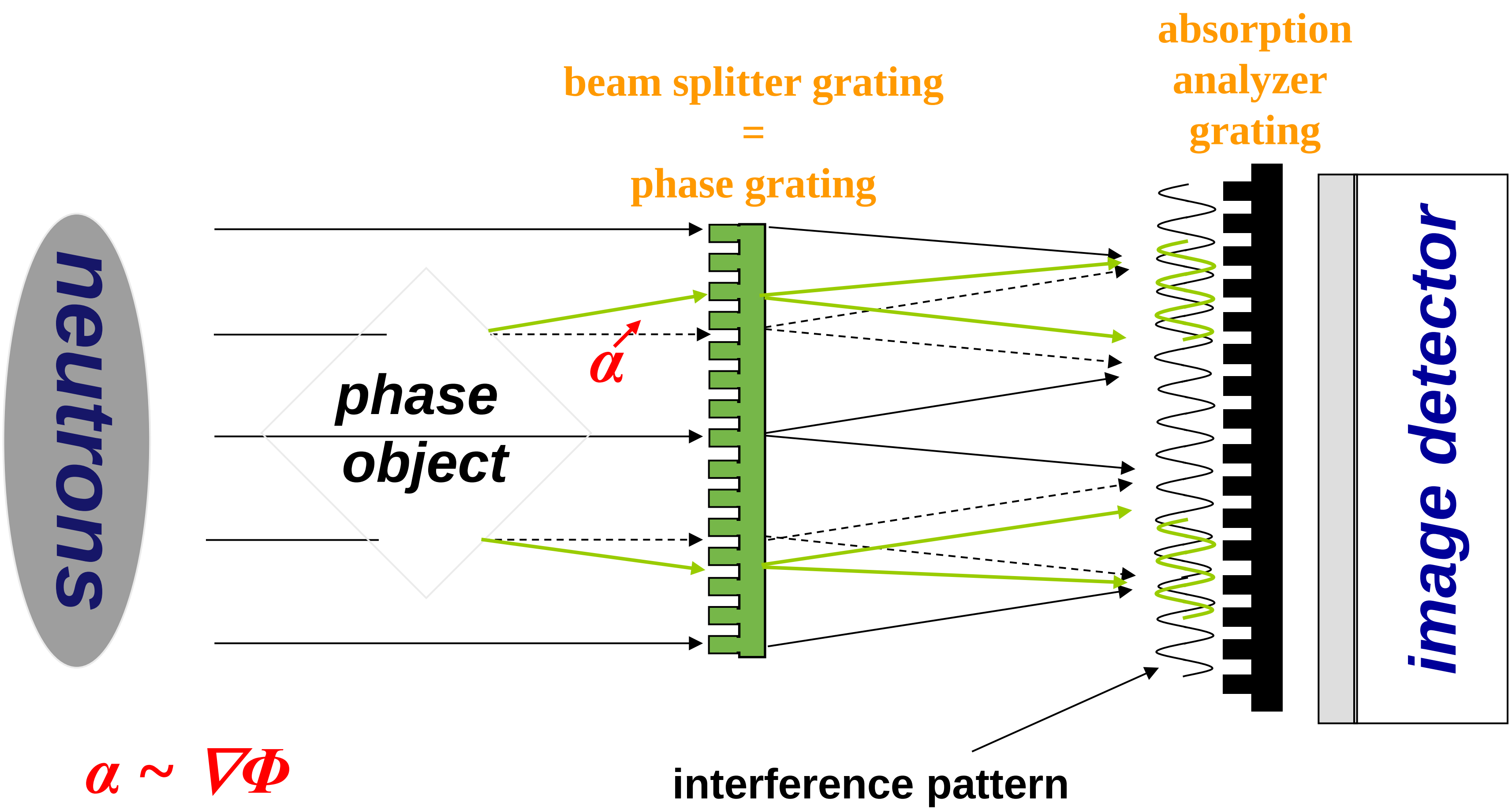

Principle:

1) to detect the local fringe position => α

2) determine from these the phase shift induced by the object

$$\alpha \Rightarrow \nabla\Phi \Rightarrow \Phi$$

neutrons

α ~

Grating interferometer

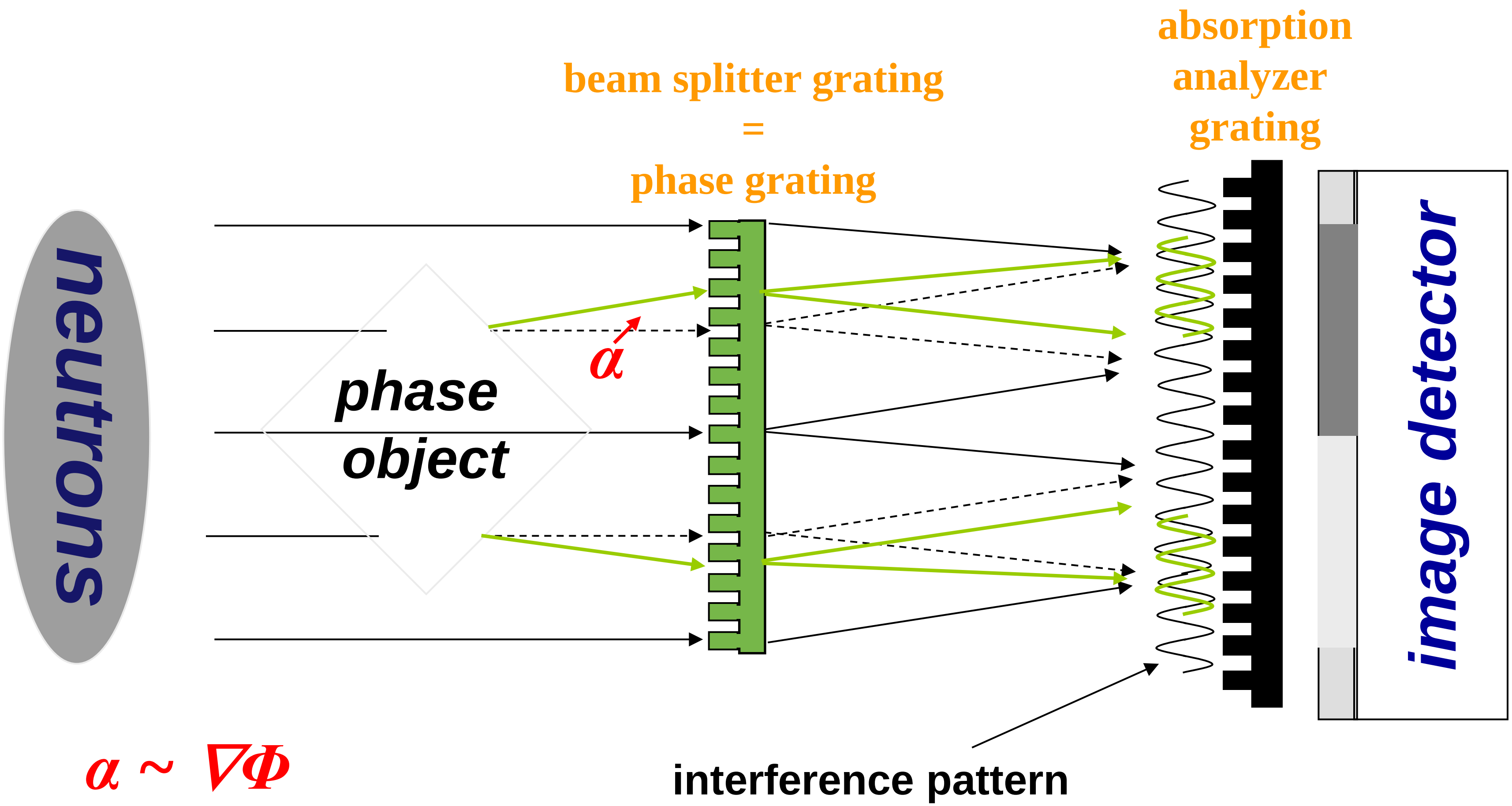

$\alpha \sim \nabla\Phi$

Grating interferometer – first results

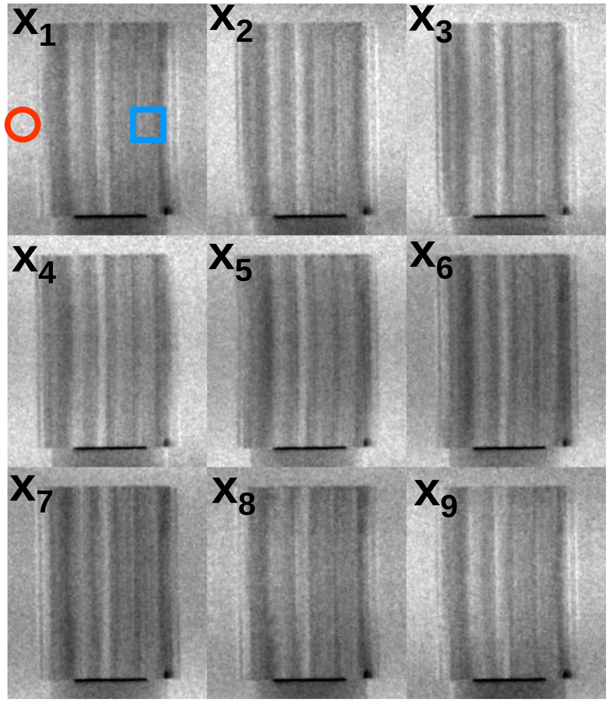

$$\phi$$

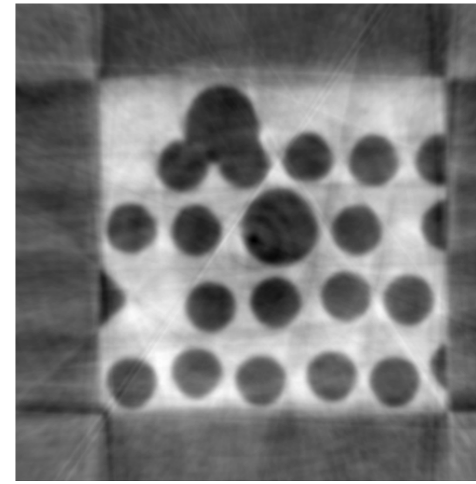

$$\vartheta \sim \frac{\partial \phi}{\partial x}$$

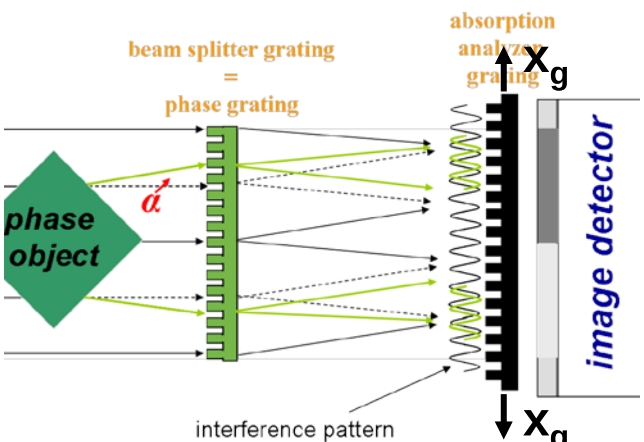

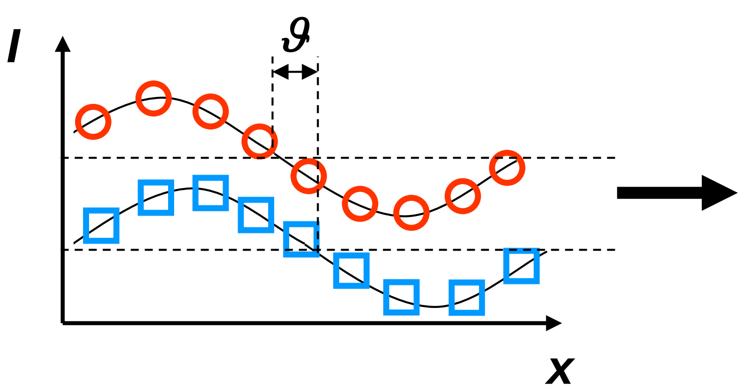

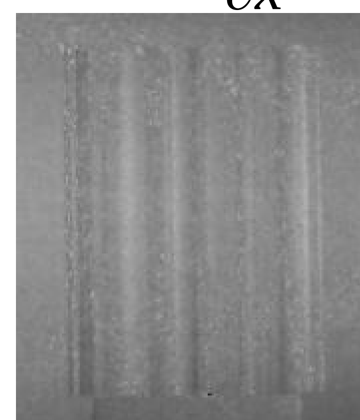

Phase/Dark-field Contrast

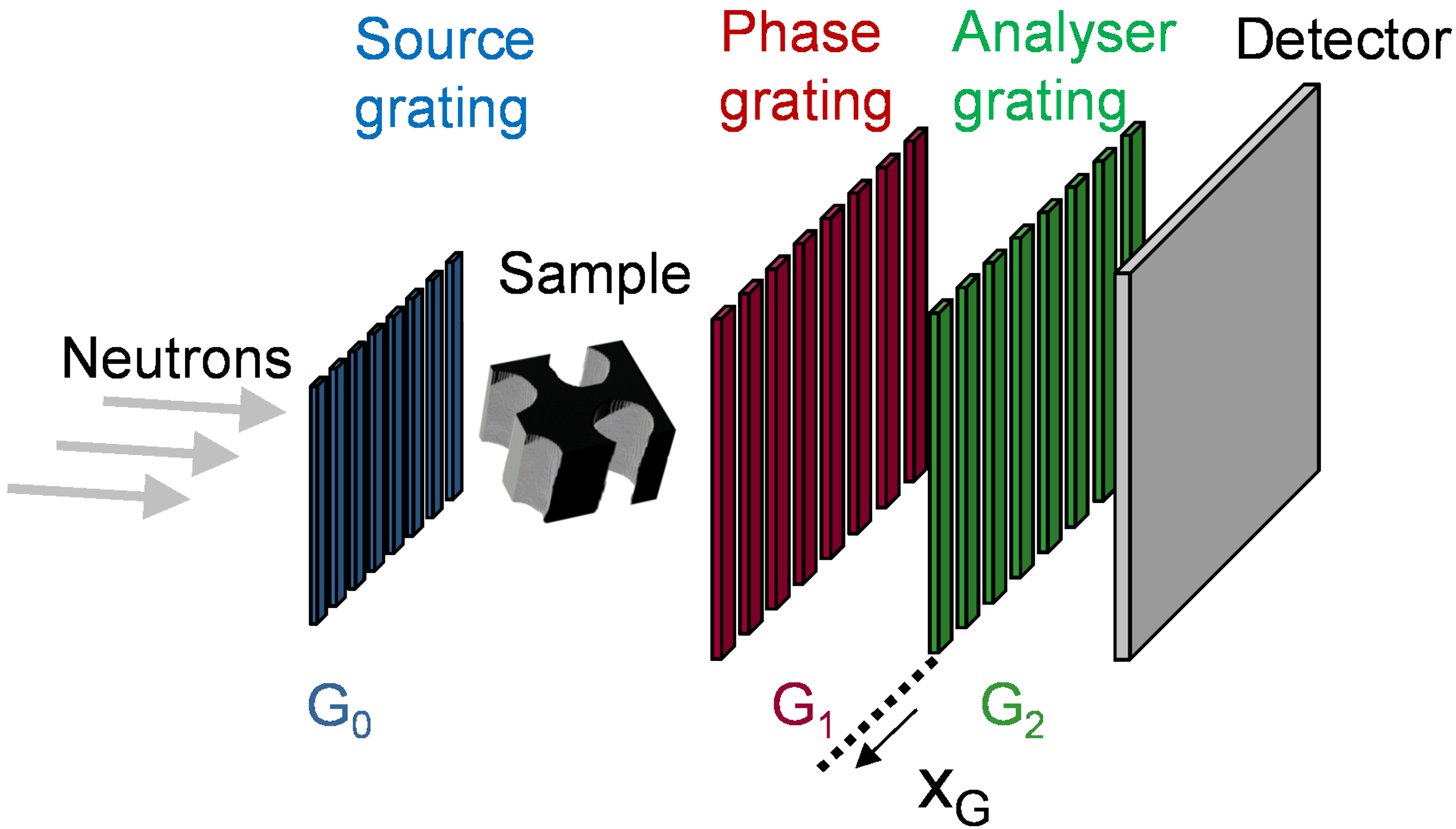

The spatially resolved analysis of the interference pattern (phase, amplitude and offset) reveal information about phase effects, small angle scattering and attenuation introduced by the sample.

Phase/Dark-field Contrast

Grating interferometry for materials science

Al-Si-binary metallic alloys
with varying hydrogen content

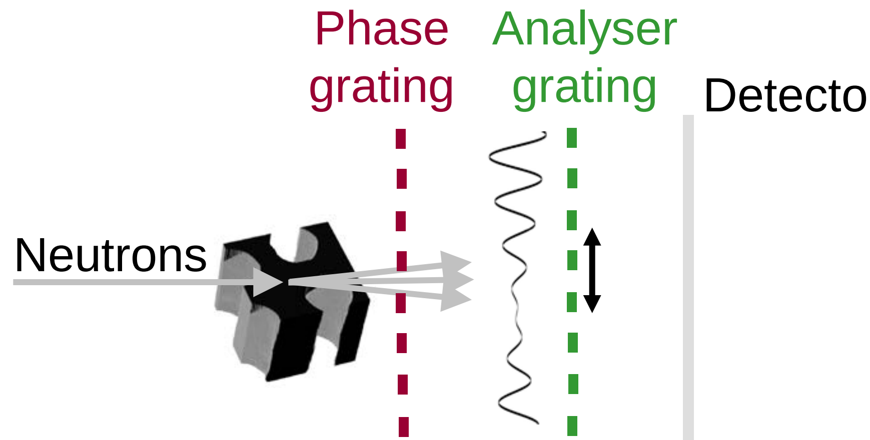

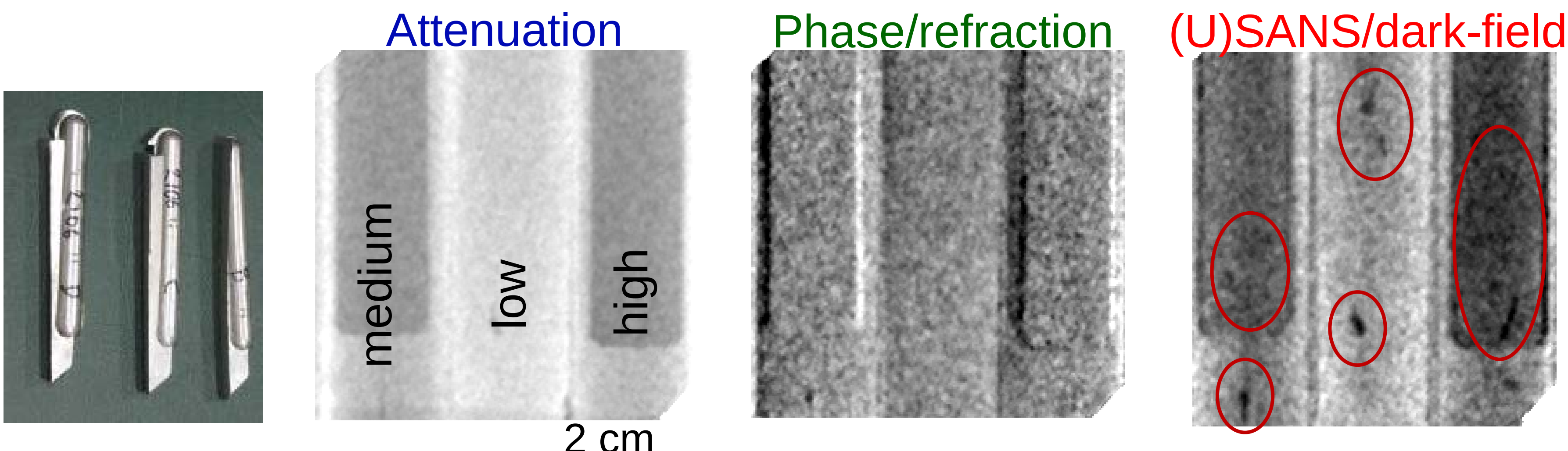

Structures (0.1–10µm)

M. Strobl et al, Neutron Dark-Field Tomography, **Physical Review Letters** 101, 123902 (2008)

Phase/Dark-field Contrast

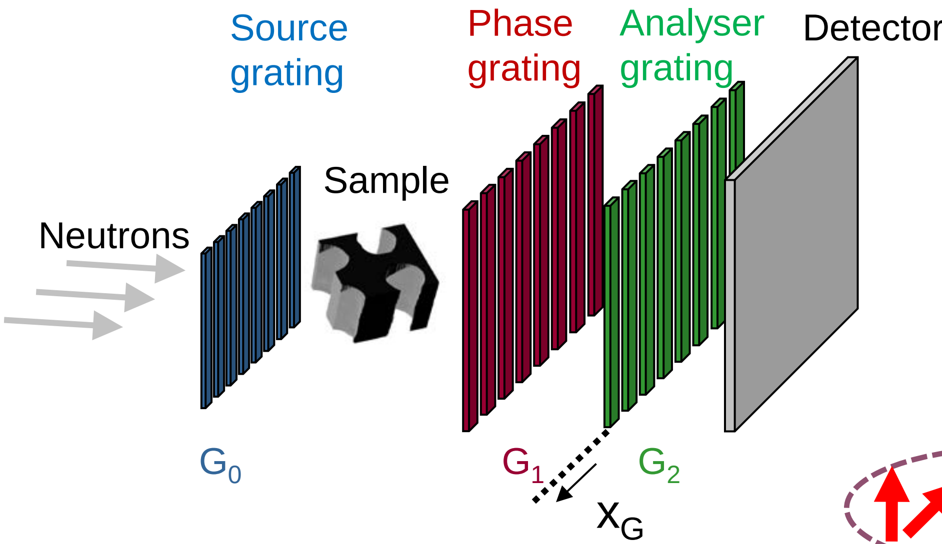

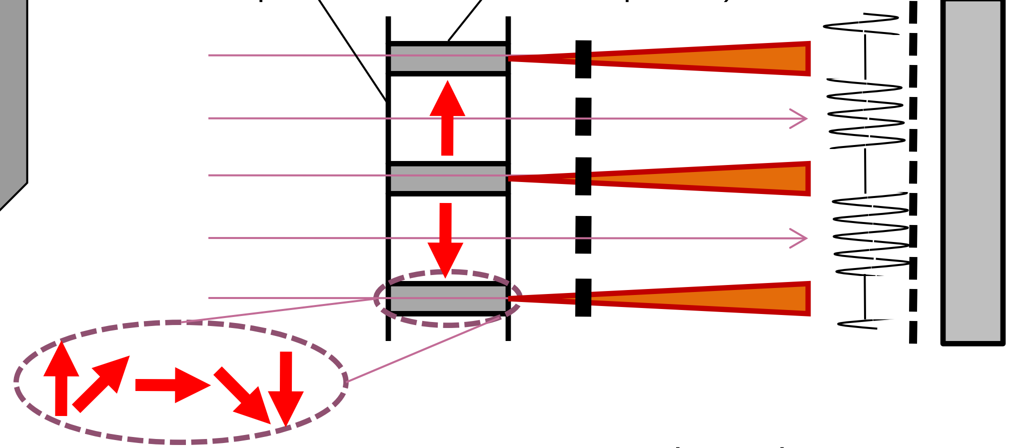

Multiple refraction at the domain walls results in local degradation of the beam coherence (decrease of the amplitude in the interference pattern).

Magnetic domains in FeSi single crystal

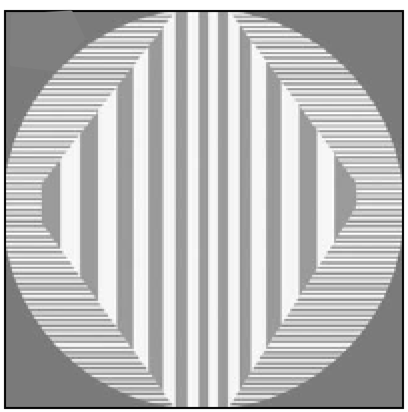

Magnetic domain structure in the sample is obtained by analyzing the amplitude of the oscillation.

Dark-field contrast

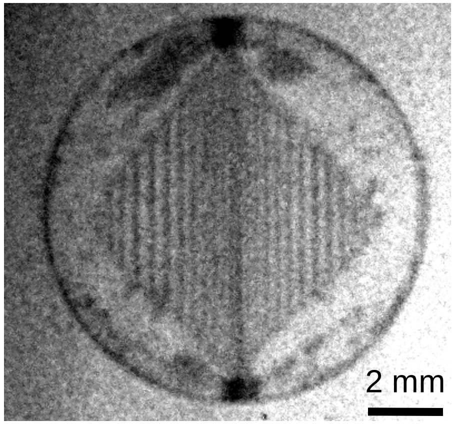

Absorption contrast (conventional radiography)

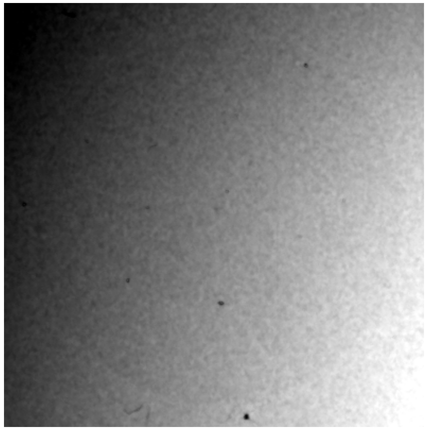

M. Strobl et al, PRL 101, 123902 (2008)

Phase/Dark-field Contrast

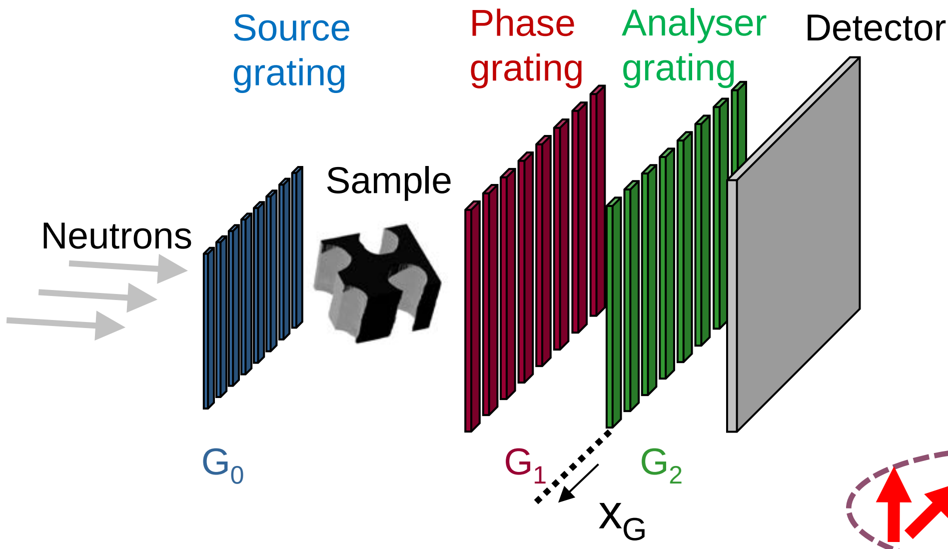

Multiple refractions at the domain walls results in local degradation of the beam coherence (decrease of the amplitude in the interference pattern).

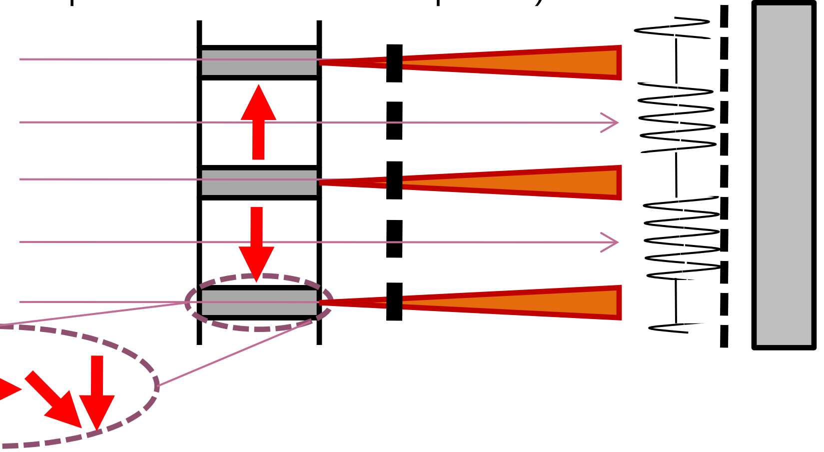

Magnetic domains in a bulky FeSi single crystal

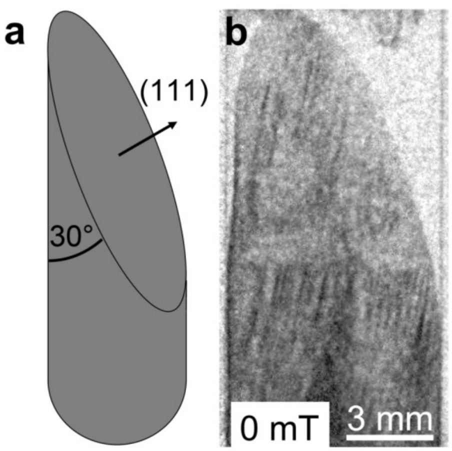

Magnetic domain structure can be visualized in 3D by applying tomographic reconstruction from 2D angular projections

3D domain distribution

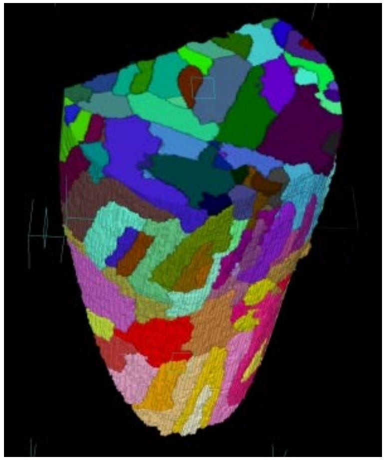

I. Manke et al, Nature Communications 1 (8), p.125 (2010)

Magnetic Contrast

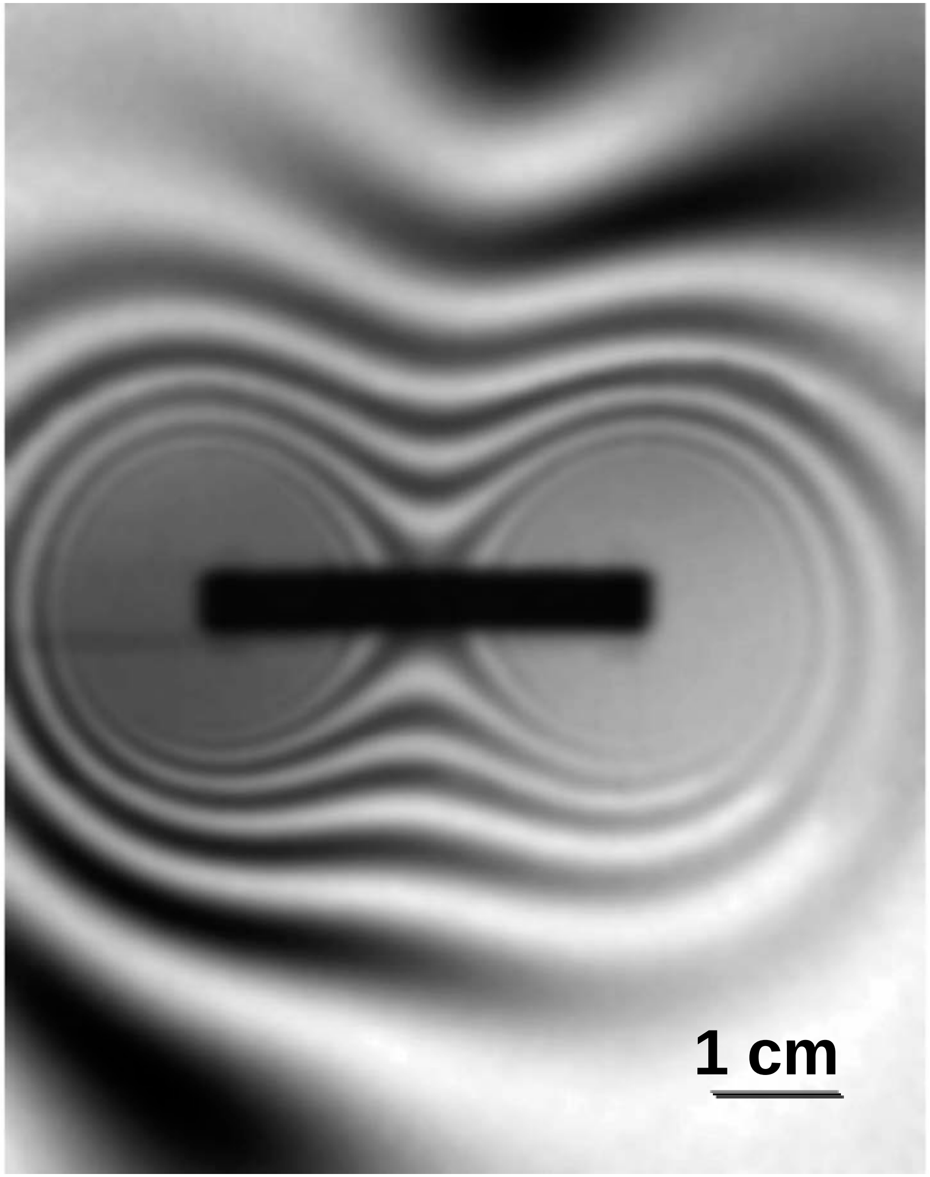

Magnetic Contrast

Principle

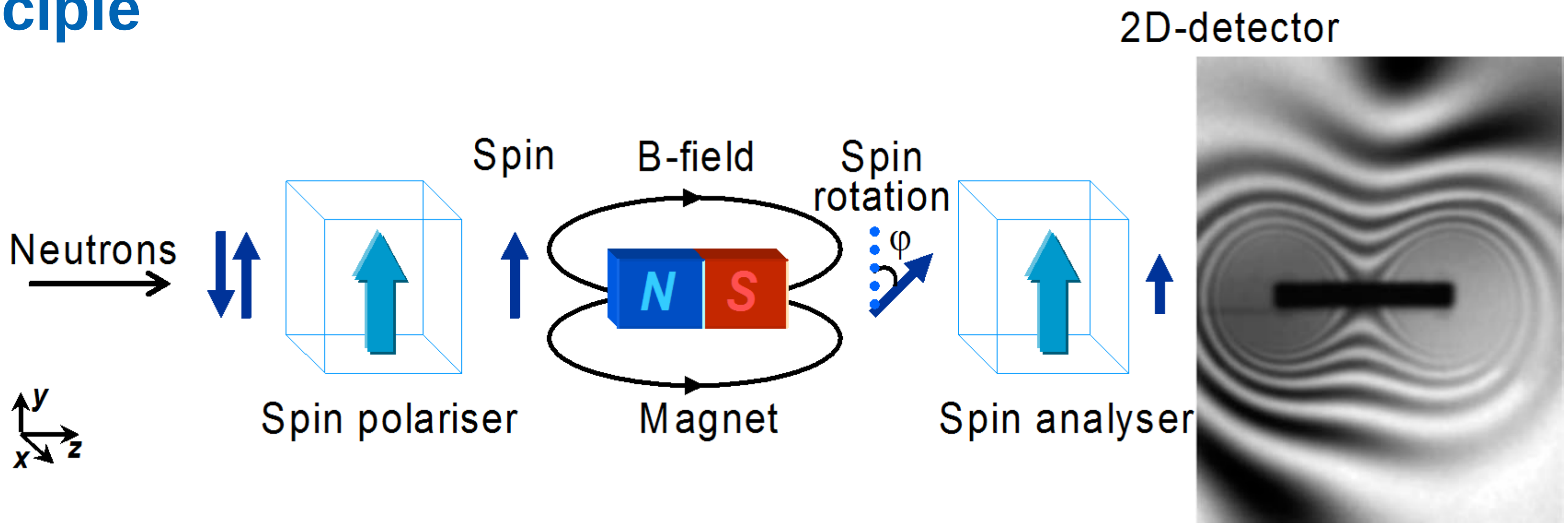

Experimental parameters

- Solid state polarazing benders
- Beam size (WxH): 20 x 4 cm^2
- Exposure times: ~10 min / image

$$\varphi = \omega_L t = \frac{\gamma_L}{v} \int_{path} H ds$$

N. Kardjilov, et al, Nature Physics 4, 399-403, (2008)

Experimental setup

Solid state polariser
Wavelength optimum λ = 3.5 Å

Refractive index: $n = 1 - \lambda^2 \left(\frac{N \cdot b_c}{2\pi} \pm \frac{\mu m B}{h^2}\right)$

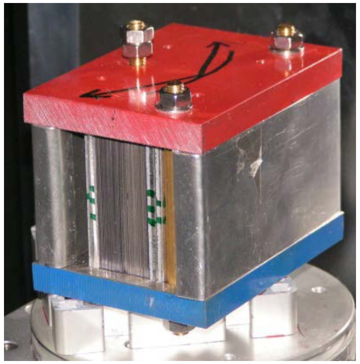

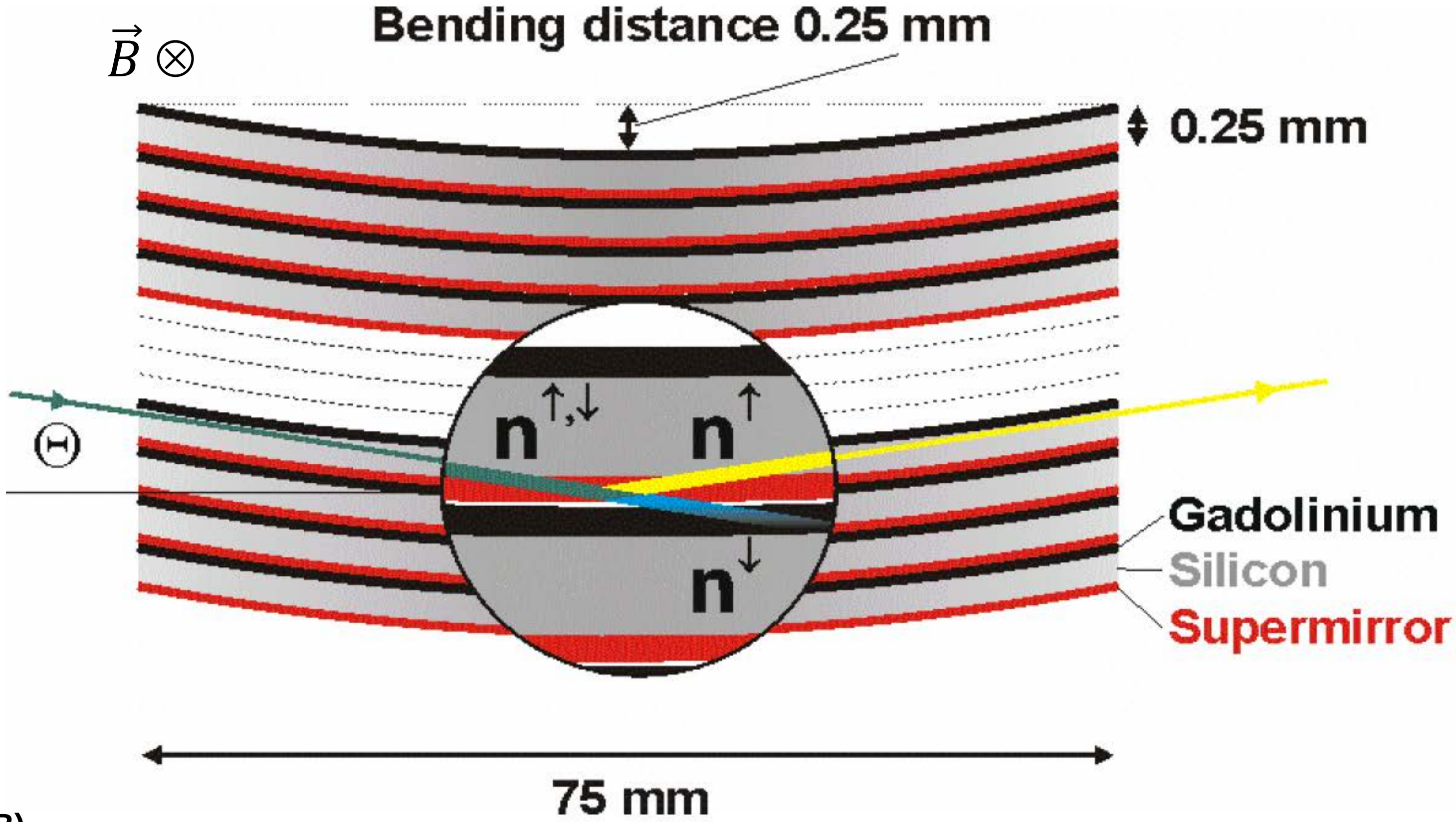

Source: Dr. Krist (HZB)

Experimental parameters

Open beam

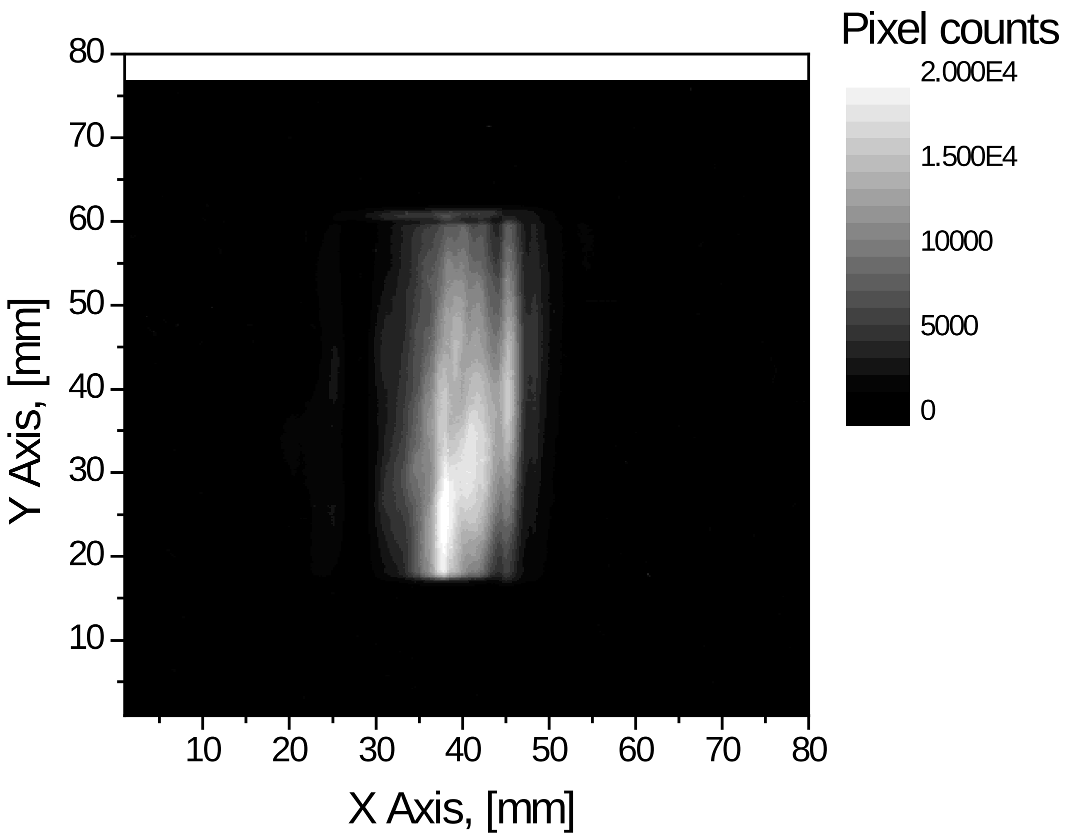

Sample

Exposure time: 300 s
Binning: 2x2

Copper coil
Wire thickness: 2 mm

Results

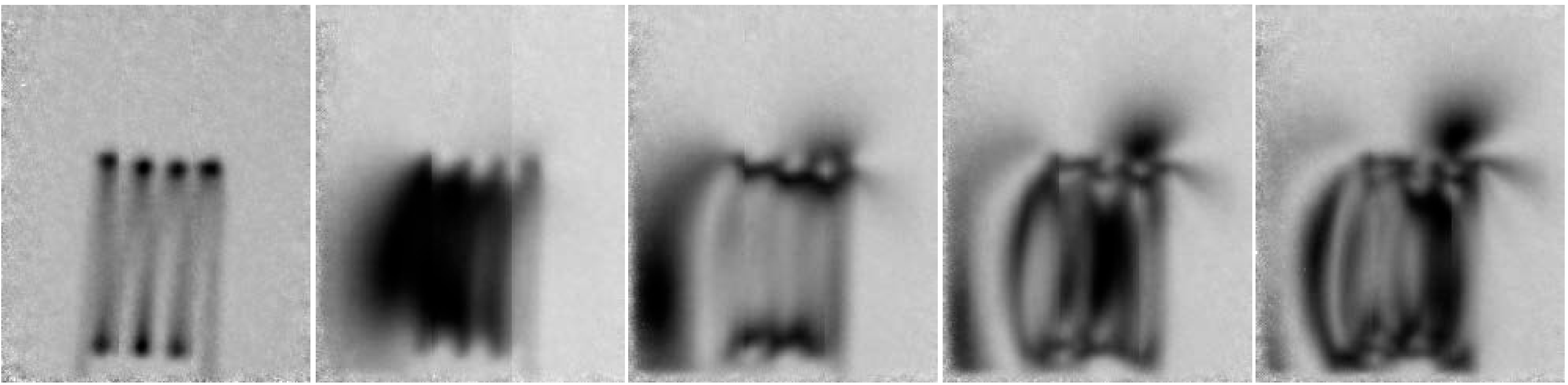

current: 0 A 4 A 8A 12 A 15 A

Scan option

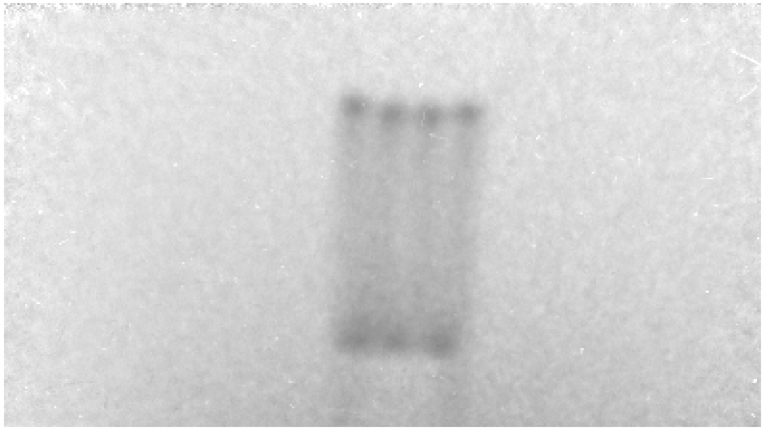

1 cm

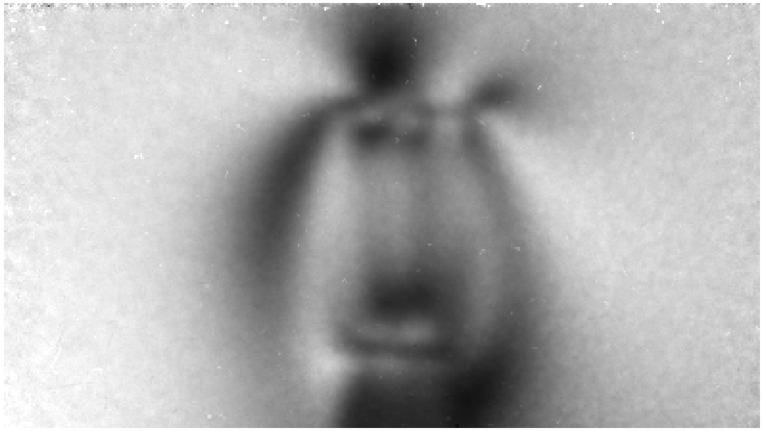

Exposure time: 1440 s (24 min)
Binning: 2x2

Neutron imaging

Principle

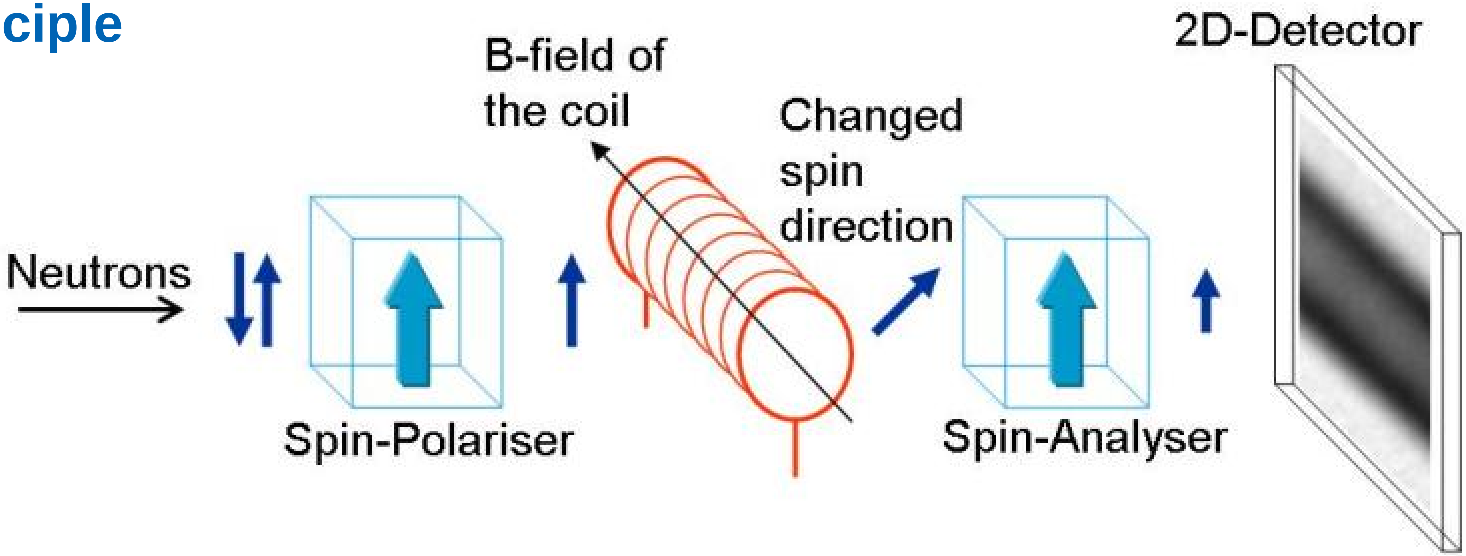

Biot-Savart law

$$d\vec{B} = \frac{\mu_0}{4\pi} \frac{I d\vec{l} \times \hat{r}}{r^2}$$

Spin rotation

$$\varphi = \frac{\gamma_L}{v} \int_{path} B ds$$

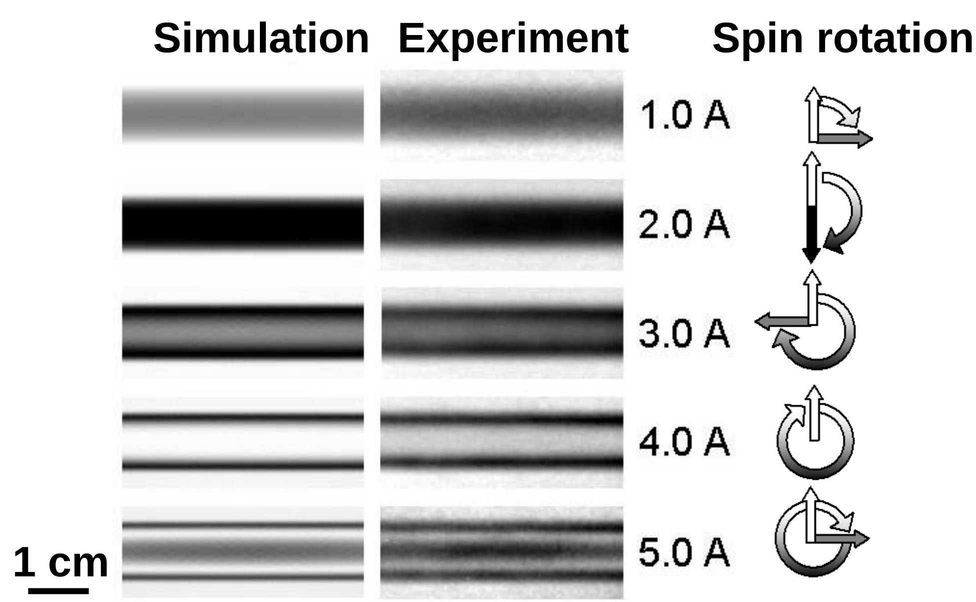

Magnetic Contrast

Flux pinning in superconductors

Pb cylinder (polycrystalline)

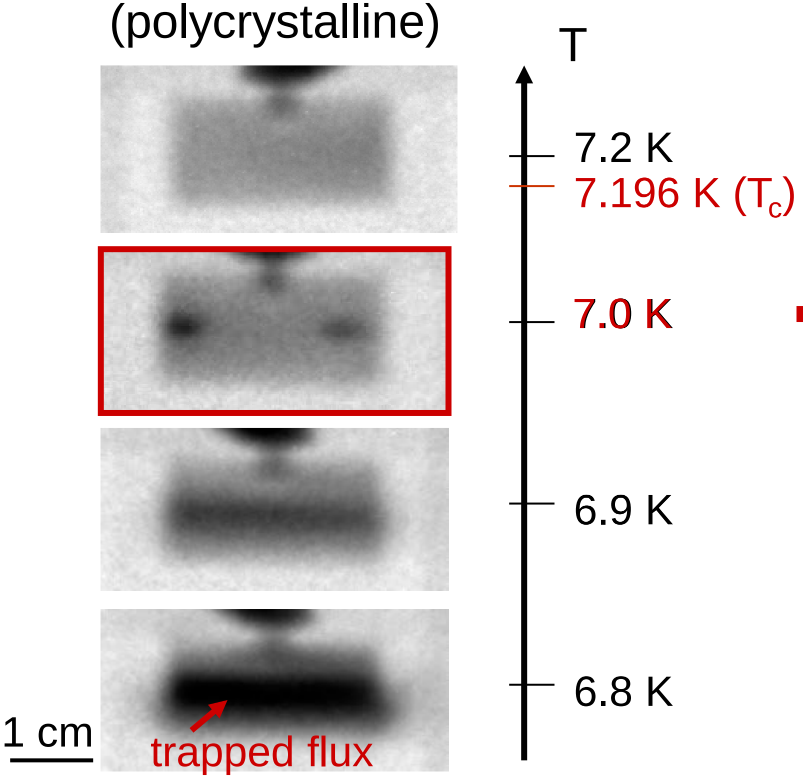

Tomography

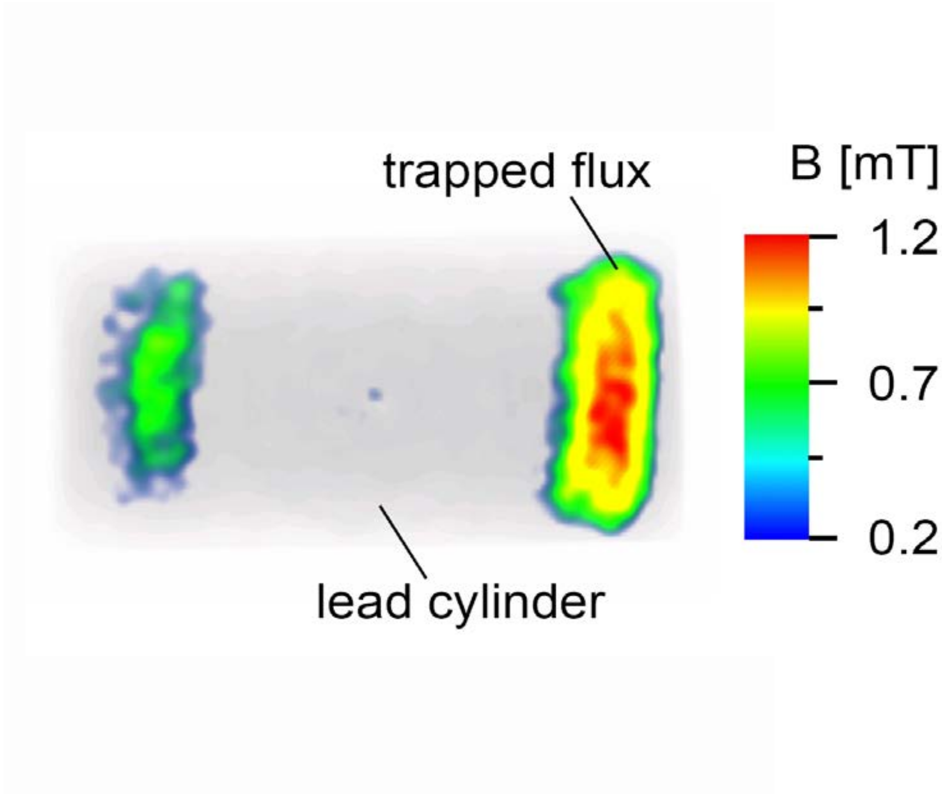

Flux pinning at cooling down below Tc while applying a homogenous magnetic field of 10 mT perpendicular to the beam.

The images were recorded after switching off the magnetic field.

Magnetic Contrast

Steps towards quantification

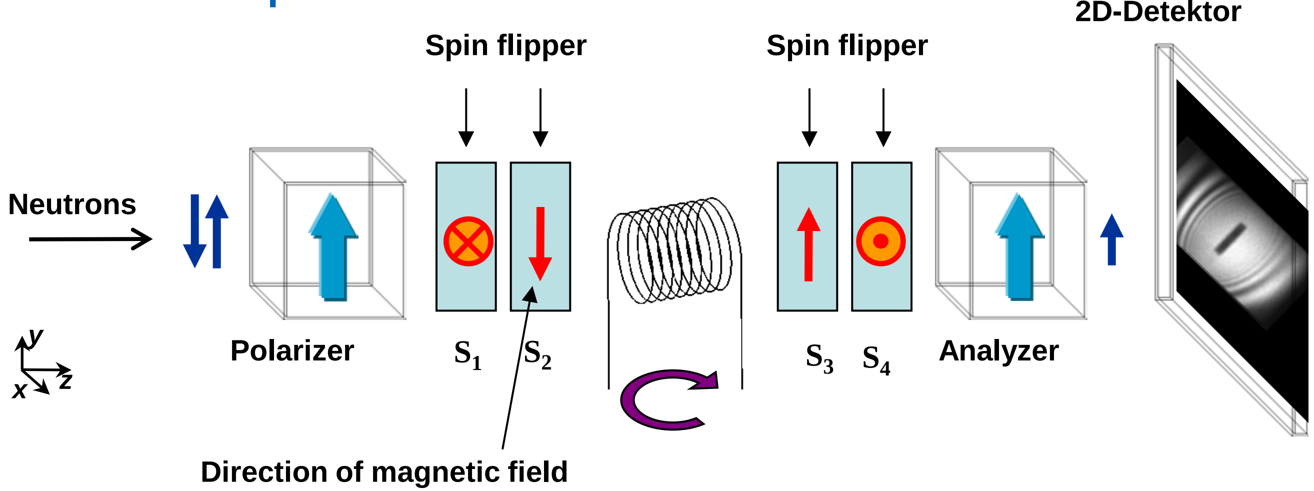

9.5 loops
I = 1.5 A
101 Projections
9+1 Tomographies

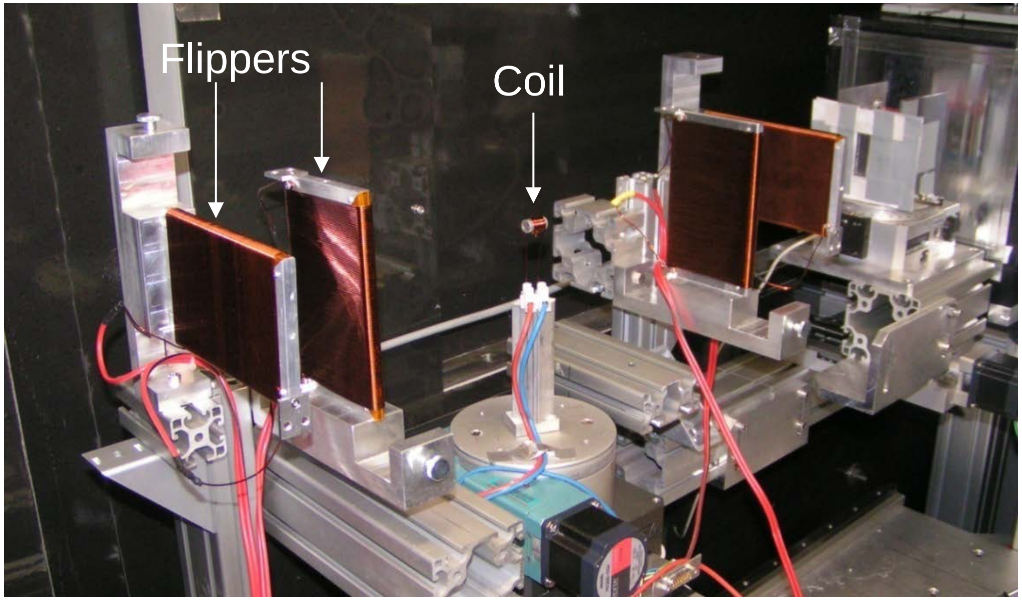

Magnetic Contrast

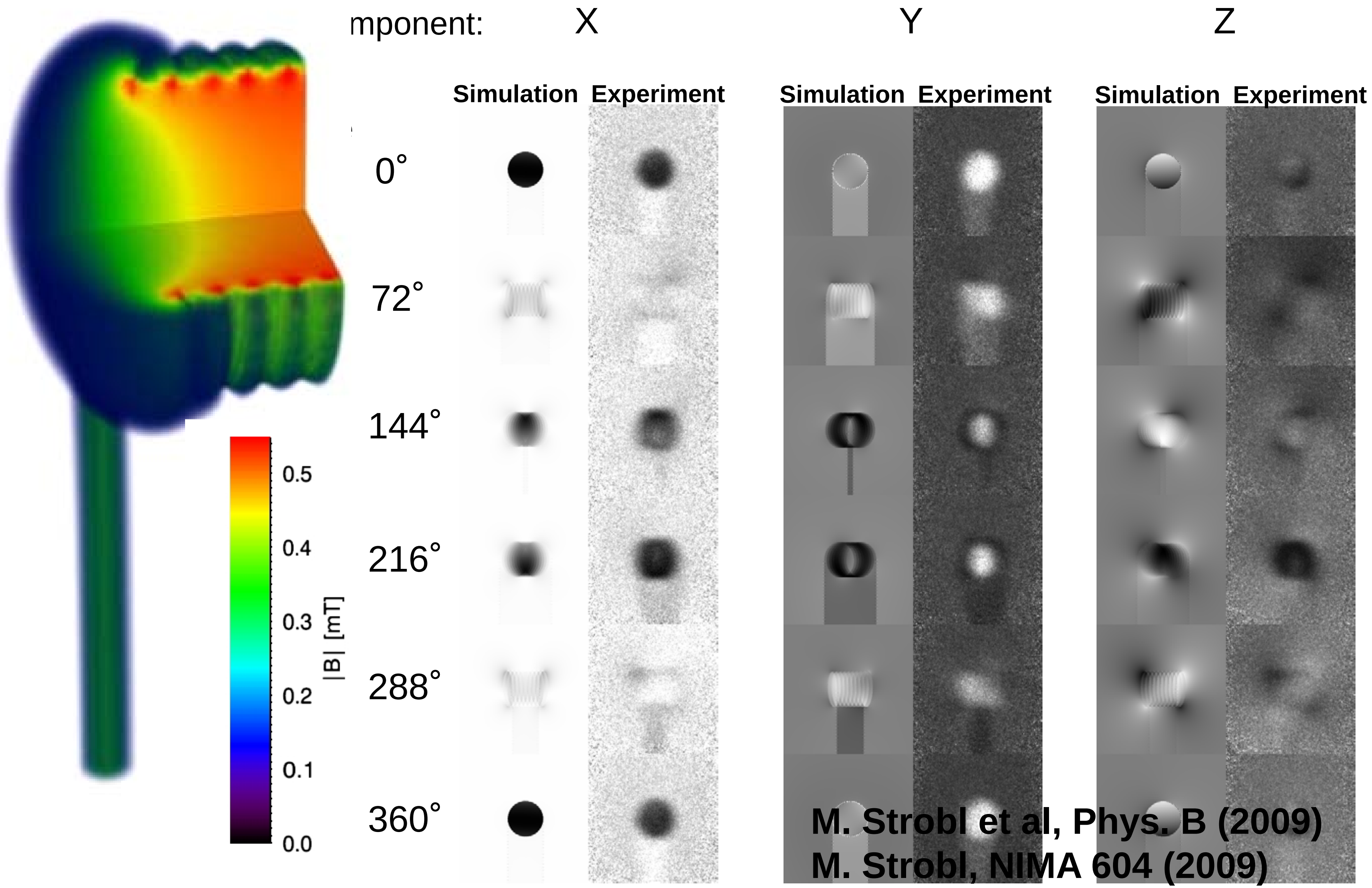

M. Strobl et al, Phys. B (2009)
M. Strobl, NIMA 604 (2009)

Magnetic Contrast

Depolarisation analysis

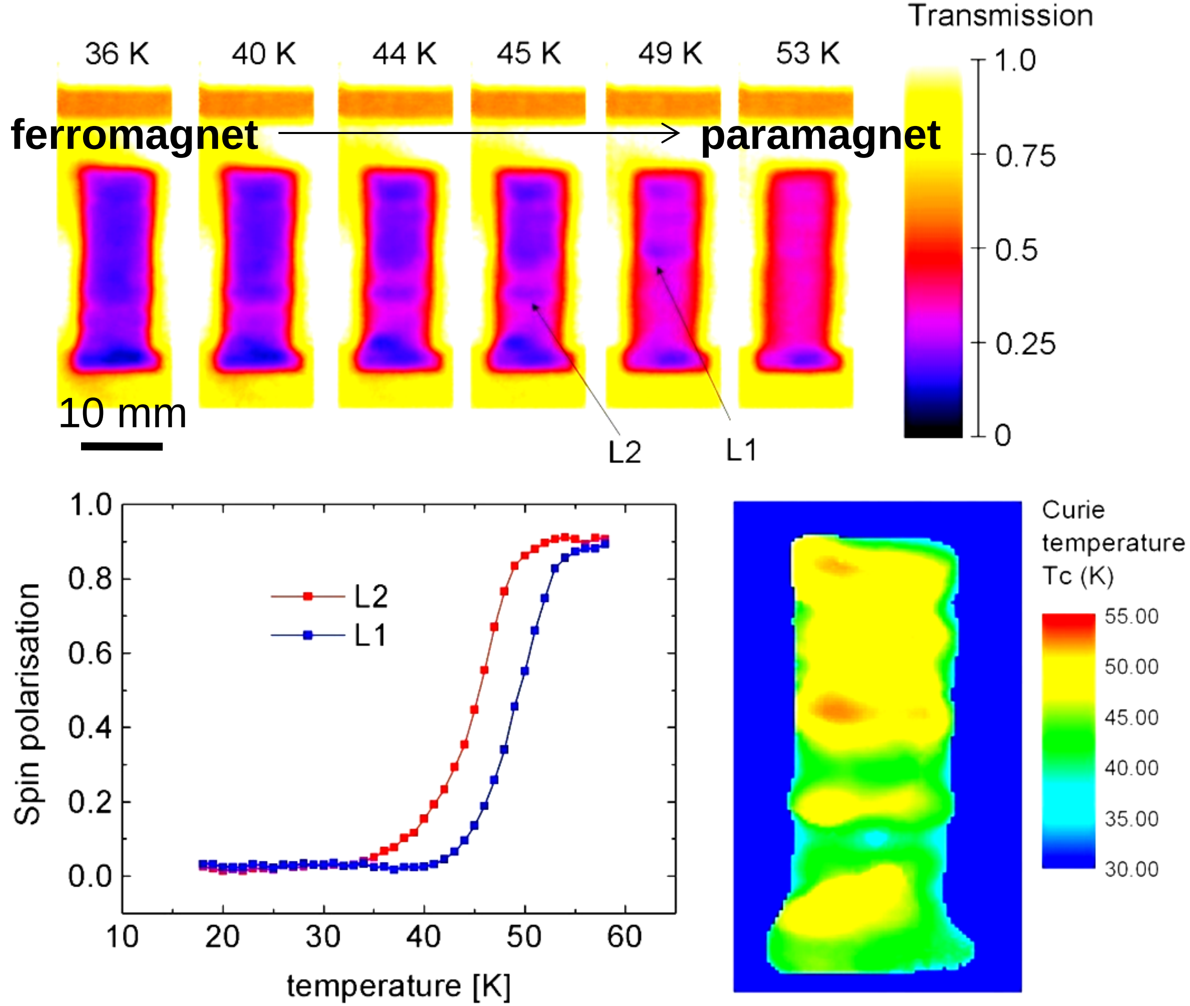

PdNi crystal (3.24% Ni) imaged by polarised neutrons

Thank you !

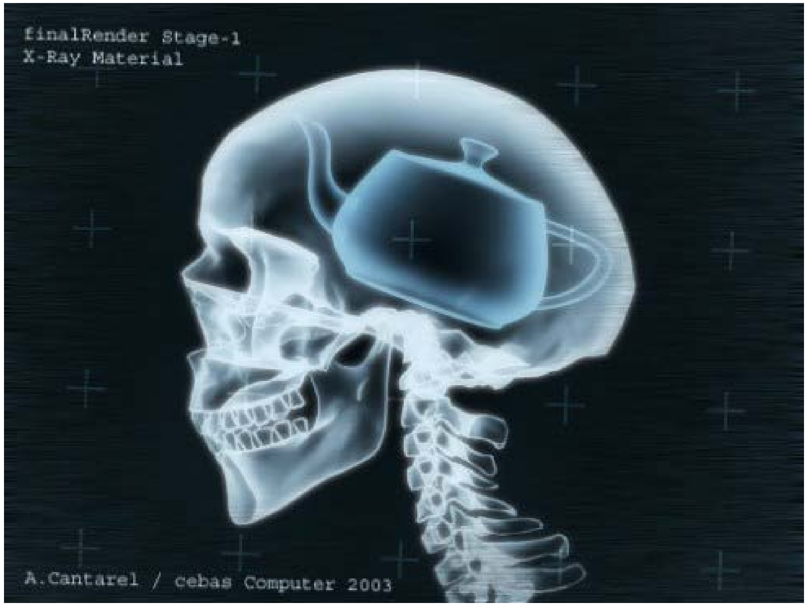
finalRender Stage-1
X-Ray Material
A.Cantarel / cebas Computer 2003